Interaction of two translational components, lysyl-tRNA synthetase and p40/37LRP, in plasma membrane promotes laminin-dependent cell migration

Dae Gyu Kim,[*,†,1] Jin Woo Choi,[*,‖,1] Jin Young Lee,[*,†,1] Hyerim Kim,[*] Young Sun Oh,[*] Jung Weon Lee,[*,†,‡] Yu Kyung Tak,[*,‡] Joon Myong Song,[*,‡] Ehud Razin,[§] Seok-Hyun Yun,[‖] and Sunghoon Kim[*,†,‡,2]

[*]Medicinal Bioconvergence Research Center and [†]College of Pharmacy, [‡]World Class University Department of Molecular Medicine and Biopharmaceutical Sciences, Seoul National University, Seoul, Korea; [§]Department of Biochemistry and Molecular Biology, The Hebrew University-Hadassah Medical School, Jerusalem, Israel; and [‖]Wellman Center for Photomedicine, Massachusetts General Hospital, Harvard Medical School, Boston, Massachusetts, USA

ABSTRACT **Although human lysyl-tRNA synthetase (KRS), an enzyme for protein synthesis, is often highly expressed in various cancer cells, its pathophysiological implications have not been understood. Here we found that KRS induces cancer cell migration through interaction with the 67-kDa laminin receptor (67LR) that is converted from ribosomal subunit p40. On laminin signal, KRS was phosphorylated at the T52 residue by p38MAPK and dissociated from the cytosolic multi-tRNA synthetase complex for membrane translocation. The importance of T52 phosphorylation for membrane translocation of KRS was confirmed by site-directed mutagenesis. In the membrane, turnover of 67LR was controlled by Nedd4-mediated ubiquitination, and KRS inhibited ubiquitin-dependent degradation of 67LR, thereby enhancing laminin-induced cell migration. This work thus unveiled a unique function of KRS in the control of cell migration and its pathological implication in metastasis.—Kim, D. G., Choi, J. W., Lee, J. Y., Kim, H., Oh, Y. S., Lee, J. W., Tak, Y. K., Song, J. M., Razin, E., Yun, S.-H., Kim, S. Interaction of two translational components, lysyl-tRNA synthetase and p40/37LRP, in plasma membrane promotes laminin-dependent cell migration. *FASEB J.* 26, 4142–4159 (2012). www.fasebj.org**

Key Words: metastasis · KRS · phosphorylation · 67LR

Aminoacyl-tRNA synthetases (ARSs) link cognate amino acids and tRNAs for protein synthesis. Interestingly, eukaryotic ARSs have unique functional domains appended to their catalytic domains, which have rendered the additional functions besides the canonical catalytic activities (1). Through these additional domains, ARSs form various functional complexes that can execute diverse cell regulatory functions (2). Owing to the functional significance of ARSs as catalysts and also as signal mediators, aberrant expression or mutations of the encoding genes can lead to various human diseases (3). Although the pathophysiological implications of ARSs in tumorigenesis have been suggested (4, 5), understanding how these enzymes are actually involved in the control of tumorigenesis is limited.

Among various protein complexes that can be formed by ARSs, the most intriguing complex is a macromolecular complex consisting of 9 different cytoplasmic ARSs and 3 nonenzymatic factors, designated aminoacyl-tRNA synthetase-interacting multifunctional protein (AIMP) 1, 2, and 3 (6–8). This complex serves as one of the protein synthesis mechanisms, and it also maintains the cellular stability of the components (9) before they are dispatched to ex-translational target sites for other functions (10). Among the components within the multi-tRNA synthetase complex (MSC), lysyl-tRNA synthetase (KRS) is the most functionally versatile and found at various cellular locations (11). For instance, in the nucleus of activated mast cells, KRS was shown to interact with transcriptional factors such as MITF for the induction of target genes (12). In addi-

Abbreviations: 37LRP, 37-kDa laminin receptor precursor; 67LR, 67-kDa laminin receptor; AIMP, aminoacyl-tRNA synthetase-interacting multifunctional protein; ARS, aminoacyl-tRNA synthetase; CID, collision-induced dissociation; ECM, extracellular matrix; EPRS, glutamyl-prolyl-tRNA synthetase; EV, empty vector; FAK, focal adhesion kinase; GST, glutathione *S*-transferase; HA, hemagglutinin; KRS, lysyl-tRNA synthetase; LR, laminin receptor; MMP-2, matrix metalloproteinase-2; MSC, multi-tRNA synthetase complex; MRS, methionyl-tRNA synthetase; si, small interfering; WRS, tryptophanyl-tRNA synthetase; WT, wild-type

[1] These authors contributed equally to this work.

[2] Correspondence: Medicinal Bioconvergence Research Center, Seoul National University, Seoul 151-742, Korea. E-mail: sungkim@snu.ac.kr

doi: 10.1096/fj.12-207639

This article includes supplemental data. Please visit *http://www.fasebj.org* to obtain this information.

0892-6638/12/0026-4142 © FASEB

tion, KRS can be secreted from some inflammatory cancer cells to induce proinflammatory cytokines, such as TNF-α (13). Although KRS was also identified in plasma membrane (11, 14–16), its functional implication has not been understood. In this work, we found that KRS is translocated to plasma membrane in a laminin-dependent manner and associates with the 67-kDa laminin receptor (67LR). The effects of the KRS-67LR interaction on cell behavior and also on the membrane stability of 67LR have been investigated in this work.

67LR is formed by dimerization of its precursor [37-kDa laminin receptor precursor (37LRP)], although the conversion process is not completely understood (17). Interestingly, 37LRP is identical to a ribosomal component, p40, that is involved in the formation of polysomes for protein synthesis (18). Whereas its precursor works in cytosol as a translational component, its dimer form, 67LR, is located in plasma membrane to mediate cell adhesion and migration through interaction with extracellular matrix, laminin (19–22). Although 67LR is not a typical laminin receptor (LR), it appears to be implicated in a few different pathological processes. For instance, it serves not only as the receptor for several pathogenic viruses (23) but is also associated with cancer metastasis (19). For this reason, understanding how its membrane turnover is regulated is important for therapeutic purposes. Here we identified KRS, an essential enzyme for protein synthesis, as a positive regulator for the membrane stability of 67LR and cell migration.

MATERIALS AND METHODS

Cell culture and materials

A549, HeLa, HCT116, MCF7, WI-26, and HEK293 cells were purchased from American Type Culture Collection (Manassas, VA, USA). The mouse mammary carcinoma 4T-1 cell line was kindly provided by Dr. Seong Jin Kim (Cha University, Gyeongghi, Korea). RPMI medium (for A549, HCT116, and 4T-1 cells) and DMEM (for other cell lines) containing 10% FBS and 1% antibiotics were used for cell cultivation. pcDNA3.1 encoding 37LRP was a kind gift from Dr. Hirofumi Tachibana (Kyushu University, Fukuoka, Japan). Myc-tagged human KRS was cloned at the *Eco*RI/*Xho*I sites of pcDNA3. The cDNA fragments encoding the indicated peptides of GFP-tagged 37LRP were cloned at *Eco*RI/*Xho*I sites of pEGFP-C2. Hemagglutinin (HA)-tagged Nedd4 (Addgene plasmid 11426) and GFP-tagged ERK (Addgene plasmid 14747) (24) were purchased from Addgene (Cambridge, MA, USA). HA-tagged JNK and pcDNA3 encoding p38MAPK were a kind gift from Dr. Eui Ju Choi (Korea University, Seoul, Korea.). Myc-tagged wild-type (WT) and C894A Nedd4 were kindly provided by Dr. Byung-Gyu Kim (Kyungpook National University, Daegu, Korea). The clones for Myc-KRS N (aa 1-219) and C (aa 220-597) fragments were kind gifts from Dr. Young Ho Jeon (Korea University, Chungnam, Korea). The cDNAs encoding Myc-KRS mutants at S49A, T52A, T388A, and T52D were cloned using a QuikChange II kit (Agilent Technologies, Santa Clara, CA, USA) following the manufacturer's instruction. GenePorter (GTS, San Diego, CA, USA) and Lipofectamine 2000 (Invitrogen, Carlsbad, CA, USA) were used as transfection reagents. Laminin (Engelbreth-Holm-Swarm murine sarcoma) was purchased from Sigma-Aldrich (St. Louis, MO, USA). The sequence for small interfering (si) RNAs targeting human KRS is as follows: si-hKRS, GCUGUUUGUCAUGAAGAAAGAGAU.

Cell migration assay

Cell migration was determined by using 24-well Transwell chambers with polycarbonate membranes (8.0-μm pore size; Costar, Cambridge, MA, USA) as described previously (13). A549 cells were suspended in serum-free RPMI medium and added to the top chamber at 1×10^5 cells/well. Extracellular matrix (ECM; 10 μg/ml; Sigma-Aldrich), laminin (10 μg/ml), collagen (10 μg/ml; Biomedical Technologies, Cambridge, MA, USA) and fibronectin (10 μg/ml, BD Biosciences, San Diego, CA, USA) were coated on the membrane. To determine the effect of extracellular KRS, purified KRS at the indicated concentration was placed in the bottom chamber. To check the effect of phosphorylation of KRS on migration, alanine mutant transfected cells were used. The cells were allowed to migrate for 6 h at 37°C in a CO_2 incubator, fixed with 70% methyl alcohol in PBS for 30 min, washed with PBS 3 times, stained with hematoxylin (Sigma-Aldrich) for 10 min, and washed with distilled water. After nonmigrant cells were removed from the top face of the membrane with a cotton swab, the membranes were excised from the chamber and mounted with Gel Mount (Biomeda, Foster City, CA, USA). The migrant cells (those attached to the bottom face of the membrane) were counted using 3 randomly selected scopes in high-power fields (×20).

Time-lapse fluorescence imaging

A549 cells were transfected with either GFP or GFP-KRS and incubated for 24 h. The cells were then replated on coverslips precoated with serum-containing culture medium for 6 h. Laminin or collagen was directly added to the medium just before live imaging using time-lapse microscopy (IX81-ZDC; Olympus, Tokyo, Japan) using a CoolSNAP HQ/QL cooled charge-coupled device digital camera (model of CoolSNAP-HQ^2). Fluorescence from the cells positive for transfection (n=10 for GFP-KRS cells with laminin, n=7 for GFP-KRS cells with collagen, and n=5 for GFP cells with laminin treatment) in a CO_2-controlled chamber was time-lapsed for 50 min with 1-min intervals at 37°C using MetaMorph 7.1.3.0 software (Molecular Devices, Sunnyvale, CA, USA). Images were analyzed for snap pictures or movies to cover images for 40 min using MetaMorph software.

Immunofluorescence staining

For activated focal adhesion kinase (FAK) staining, A549 cells were fixed in 3.8% paraformaldehyde for 5 min at room temperature, permeabilized with 0.05% Triton X-100 for 5 min, rinsed in PBS, and blocked in PBS containing 2% BSA for 30 min. Then, the cells were incubated with primary antibody against phospho-Y397 FAK for 1 h at room temperature. Actin was stained by using rhodamine phalloidin (Invitrogen). To confirm that the phosphorylation of KRS affects the localization in membrane, A549 cells transfected with GFP-KRS WT, T52D, and T52A were used. Transfected A549 cells were treated with laminin or not treated and then were fixed with methyl alcohol and stained with DAPI. After a wash with cold PBS, the samples were mounted. The mounted samples were visualized by fluorescent microscopy (BX51 fluorescent microscope; Olympus). For the staining of endogenous KRS and 67LR, A549 cells on a 9-mm coverslip were fixed with 70% methyl alcohol and washed briefly with

cold PBS. After incubation with the blocking buffer containing 1% CAS-Block (00-8120; Invitrogen), 3% BSA, and 0.5% Triton X-100 for 30 min, the cells were incubated for 1 h with the antibodies against KRS and 67LR (MLuC-5; Santa Cruz Biotechnology, Inc., Santa Cruz, CA, USA) that were conjugated with Alexa 488 and 555 (Invitrogen), respectively. After being washed with cold PBS for 30 min, the specimens were observed by laser scanning microscopy.

Quantum dot analysis

To monitor the extracellularly exposed domain of KRS, KRS cDNA was inserted at *Eco*RI/*Sal*I sites of pEGFP-N3 and pEGFP-C2 (Clontech, Mountain View, CA, USA) to generate GFP fused to the C- and N-terminal ends of KRS, respectively. A549 cells transfected with pEGFP-N3, pEGFP-N3-KRS, pEGFP-C2, or pEGFP-C2-KRS were incubated in the absence and presence of laminin, rinsed with PBS, and incubated with anti-GFP antibody (Santa Cruz Biotechnology) at room temperature. After 1 h of incubation, the cells were washed with PBS, treated with the biotinylated anti-mouse IgG antibody (eBioscience, San Diego, CA, USA) and QD625-streptavidin conjugates (Invitrogen) for 1 h at room temperature. Finally, the immunostained cells were rinsed with PBS. Image analysis of the immunostained cells was accomplished using a custom-made hyperspectral single cell imaging cytometer. The setup and working principle of the imaging system were described previously (25, 26). The acquired cellular images were processed and analyzed using MetaMorph.

FAK assay

A549 cells transfected with empty vector (EV) or KRS for 48 h were incubated for 12 h in normal serum-containing culture medium and replated on the laminin-precoated (10 μg/ml) culture dishes. The cells were detached, suspended with serum-free culture medium containing 1% BSA (Sigma-Aldrich), and rolled over (60 rpm in CO_2 incubator) for 1 h to nullify the basal signaling activity. The cells were either kept in suspension or reseeded onto the laminin-precoated culture dishes containing the replating medium and incubated in a CO_2 incubator for 2 h. The cells were harvested, and the proteins were extracted for Western blot analysis with the primary antibodies against phospho-Y397FAK, phospho-Y925FAK, FAK (Abcam, Cambridge, MA, USA), KRS (Abcam), and tubulin (Sigma-Aldrich).

Zymography

A549 cells transfected with si-control and si-KRS or EV and Myc-KRS were incubated for 48 and 24 h, respectively, and seeded (1×10^5 cells/well). After cells were starved in serum-free RPMI medium for 2 h, laminin (10 μg/ml) was added and incubated for 24 h. The culture medium (20 μl) was mixed with 5× FOD buffer (0.125 M Tris-HCl, pH 6.8; 4% SDS; 20% glycerol; and 0.01% bromphenol blue) and subjected to 10% SDS-PAGE containing 1 mg/ml gelatin. The gel was washed with 2.5% Triton X-100 twice for 20 min per washing and then with distilled water twice for 20 min per washing and incubated with the reaction buffer (50 mM Tris-HCl, pH 7.5; 10 mM $CaCl_2$; 150 mM NaCl; 1 μM $ZnCl_2$; 1% Triton X-100; and 0.002% sodium azide) for 24 h at 37°C. The gel was washed with distilled water, stained with Coomassie Blue R250, and then destained with 35% methanol.

Yeast 2-hybrid analysis

The cDNA encoding human KRS was obtained by PCR with the forward and backward primers containing *Eco*RI and *Xho*I sites, respectively. The product was digested with *Eco*RI and *Xho*I and ligated to the corresponding sites of pEG202 (for the construction of LexA fusion proteins). Likewise, the cDNAs for AIMP1/p43, AIMP2/p38, and 37LRP were inserted into pJG4-5 (for the construction of B42 fusion proteins). The cDNA encoding human 37LRP was kindly provided by Dr. Barbara J. Ballermann (University of Alberta, Edmonton, AB, Canada). The positive interaction was determined by the formation of blue colonies on the X-gal-containing yeast medium.

Immunoprecipitation

A549 cells were lysed with 20 mM Tris-HCl (pH 7.4) buffer containing 150 mM NaCl, 0.5% Triton X-100, 0.1% SDS, and protease inhibitor (Calbiochem, San Diego, CA, USA). The protein extracts were incubated with normal IgG and protein G agarose for 2 h and then were centrifuged to remove nonspecific IgG binding proteins. We mixed the supernatants with purified anti-KRS antibody, incubated the mixture for 2 h at 4°C with agitation, added protein A agarose, and centrifuged. After being washed with cold lysis buffer 3 times, the precipitates were dissolved in the SDS sample buffer and separated by SDS-PAGE. To determine binding of KRS and LR in different cell fractions, we transfected Myc-tagged KRS and separated plasma membrane and cytosolic fractions using a ProteoExtract kit (Calbiochem) following the manufacturer's instruction. To analyze protein levels, extracts from the cells were separated by 10% SDS-PAGE. Anti-LR antibody (ab2508; Abcam) was used for simultaneous immunoblotting of 37LRP and 67LR, unless specified. Antibodies for HSP90 and pan-cadherin were purchased from Santa Cruz Biotechnology, Inc.

***In vitro* binding assay**

Human 37LRP/p40 was prepared by *in vitro* translation in the presence of [^{35}S]methionine and mixed individually with glutathione *S*-transferase (GST), GST-KRS, and GST-tryptophanyl-tRNA synthetase (WRS). GST proteins were precipitated with glutathione-Sepharose, and 37LRP coprecipitated with GST proteins was detected by autoradiography. To determine the domains of LR involved in the interaction with KRS, the DNA fragments encoding the indicated domains of 37LRP were isolated by PCR and expressed as GFP fusion proteins. They were then mixed with GST-KRS and precipitated with glutathione-Sepharose. Coprecipitates of the LR fragments were determined by Western blotting with antibody against GFP.

Flow cytometry

To determine the laminin-induced surface exposure of KRS and methionyl-tRNA synthetase (MRS), A549 cells transfected with Myc-KRS or Myc-MRS were detected with anti-Myc antibody. For quantification of 67LR on the cell surface, 1×10^6 cells were incubated with IgG or anti-LR antibody (MLuC5; 1 μg) recognizing the extracellular domain of 67LR and then with FITC secondary antibody. After being washed with PBS, the samples were scanned by FACS. The antibodies against integrin α2 (1 μg; Chemicon International, Temecula, CA, USA), α3 (1 μg; GenScript, Piscataway, NJ, USA), α4 (1 μg; Chemicon International), α5 (1 μg; Chemicon International), α6 (1 μg; Chemicon International), β4 (27), and αvβ5 (1 μg; Chemicon International) were used to determine the effect of KRS on surface exposure of integrins.

Pulse-chase experiment

HEK293 cells transfected with si-KRS or si-control (Stealth RNAi Negative Control Medium GC Duplex, 12935-300; Invitrogen) were then incubated with methionine-free medium for 1 h. Then [^{35}S]methionine (50 μCi/ml) was added and incubated for 1 h. After the radioactive methionine was washed off with fresh medium, 67LR was immunoprecipitated with its specific antibody (Santa Cruz Biotechnology), separated by 12% SDS-PAGE, and subjected to autoradiography using a BAS scanner (FLA-3000; Fujifilm, Tokyo, Japan).

Fatty acylation

To see the effect of KRS on fatty acylation of LR, A549 cells with different expression levels of KRS were washed 3 times with PBS, starved with serum-free medium for 4 h, and then pulsed for 2 h in medium containing 0.1 mCi/ml palmitic acid. The cells were washed 3 times with cold PBS and incubated with laminin in serum-free medium for 1 h. LR was immunoprecipitated with antibody against LR (Abcam). The radioactivities of the precipitates were measured by a liquid scintillation counter (Wallac, Turku, Finland).

In vitro kinase assay

A549 cells were incubated with SB202190 (20 μM; Calbiochem) or LY294002 (20 μM, Calbiochem) for 4 h and treated with laminin for 1 h. The cells were washed with cold PBS 3 times and lysed by sonication in the kinase buffer containing 20 mM Tris-HCl, pH 7.5; 15 mM $MgCl_2$; 1 mM EGTA; 0.1 mM DTT; 1 mM Na_3VO_4; 0.5 mM NaF; 0.1 mM β-glycerophosphate; and 0.1 mM sodium pyrophosphate. After purified GST-KRS and GST were preincubated with cold ATP (250 μM) on ice for 10 min, they were mixed with the protein extract (250 μg) or p38MAPK (Cell Sciences, Canton, MA, USA) and 10 μCi (3000 Ci/mmol) [γ-^{32}P]ATP in the kinase buffer, and incubated at 30°C for 30 min, and the incubation was stopped by the addition of the SDS sample buffer. The proteins in the reaction mixture were separated by SDS-PAGE and autoradiographed (FLA-3000; Fujifilm).

Mass spectrometry

Coomassie-stained KRS phosphorylated by recombinant p38MAPK was in gel-digested with trypsin (Promega, Madison, WI, USA) and analyzed by capillary column liquid chromatography-tandem mass spectrometry analysis to map the peptides and identify phosphopeptides. The experiments were done using LTQ-Orbitrap mass spectrometry systems (Thermo Finnigan, San Jose, CA, USA) equipped with nanospray ionization sources. Data were acquired in data-dependent mode to simultaneously record full-scan mass and collision-induced dissociation (CID) spectra with multistage activation. For peptide mapping, the CID spectra were compared to the sequence of human KRS using Sequest (Bioworks; Thermo Electron, Waltham, MA, USA). To identify phosphopeptides and specific phosphorylation sites, CID spectra were searched for the peptides that contain phospho (p)-Ser, p-Thr, or p-Tyr modifications by a combination of database searches and by plotting neutral loss chromatograms to show characteristic loss of a phosphate group.

Ubiquitination assay

A549 cells transfected with the indicated plasmids were preincubated with MG132 (50 μM) and cultivated in the presence of laminin. 67LR was immunoprecipitated with anti-LR antibody (MLuC5), and the precipitates were separated by SDS-PAGE for immunoblotting.

RT-PCR

Total RNAs were extracted from A549 cells that were dose dependently transfected with KRS or treated with laminin time dependently using an RNeasy Mini Kit (Qiagen, Valencia, CA, USA). Then 1 μg of RNA was used for RT-PCR with dNTP, random hexamer, and Moloney murine leukemia virus in 20 μl of reaction mixture, and 1 μl of cDNA was used for PCR with appropriate primers using PCR PreMix (Bioneer Corporation, Alameda, CA, USA). The sequences for the primers specific to 37LRP, KRS, GAPDH, and actin are the following: 37LRP, CCGCTCGAGATGTCCGGAGCCCTTGATGTCCTG and CCGGGATCCTTAAGACCAGTCAGTGGTTGCTCC; KRS, CAATGCCCATGCCCCAGCCA and ACCCCACCCTTCCGGCGAAT; GAPDH, TTTGGTCGTATTGGGCGCCTG and CCATGACGAACATGGGGGCAT; and actin, CCTTCCTGGGCATGGAGTCCT and GGAGCAATGATCTTGATCTT.

Detection of secreted KRS

A549 cells were cultivated in complete medium to 70% confluence and then were washed twice with PBS and further cultivated in serum-free medium in the presence of laminin (10 μg/ml) for 4 h. The culture medium was collected and centrifuged at 500 *g* for 10 min and then at 10,000 *g* for another 30 min to remove contaminants. The proteins were precipitated from the supernatants with 12% trichloroacetic acid for 1 h at 4°C and then were centrifuged at 18,000 *g* for 15 min. The pellets were resuspended with 100 mM HEPES buffer (pH 8.0) and separated by 10% SDS-PAGE. The secreted KRS was determined by Western blotting with anti-KRS antibody.

Effect of extracellular KRS on the membrane residence of 67LR

The purified recombinant human KRS was prepared as described previously (13). To determine the effect of extracellular KRS on the membrane level of 67LR, A549 cells were incubated with the purified KRS (100 nM) or laminin (10 μg/ml) in serum-free medium for 1 h. A549 cells were also transfected with Myc-KRS and cultivated for 24 h. A549 cells were then preincubated with the purified KRS (100 nM) in serum-free medium for 1 h and further cultivated in the presence of laminin (10 μg/ml) for 1 h. The cells were harvested, washed with cold PBS 3 times, and divided into cytosol and membrane fractions. The proteins in each fraction were separated by SDS-PAGE, and the amounts of 67LR and KRS were detected by Western blotting with anti-67LR and anti-KRS antibodies, respectively.

RESULTS

KRS mediates laminin-induced cell migration

Although KRS is often highly expressed in various cancer cells and tissues, its pathophysiological meaning is not understood. To have functional insight into the increased expression of KRS in cancer cells, we have changed the expression level of KRS by exogenous supplementation and siRNA-mediated knockdown methods

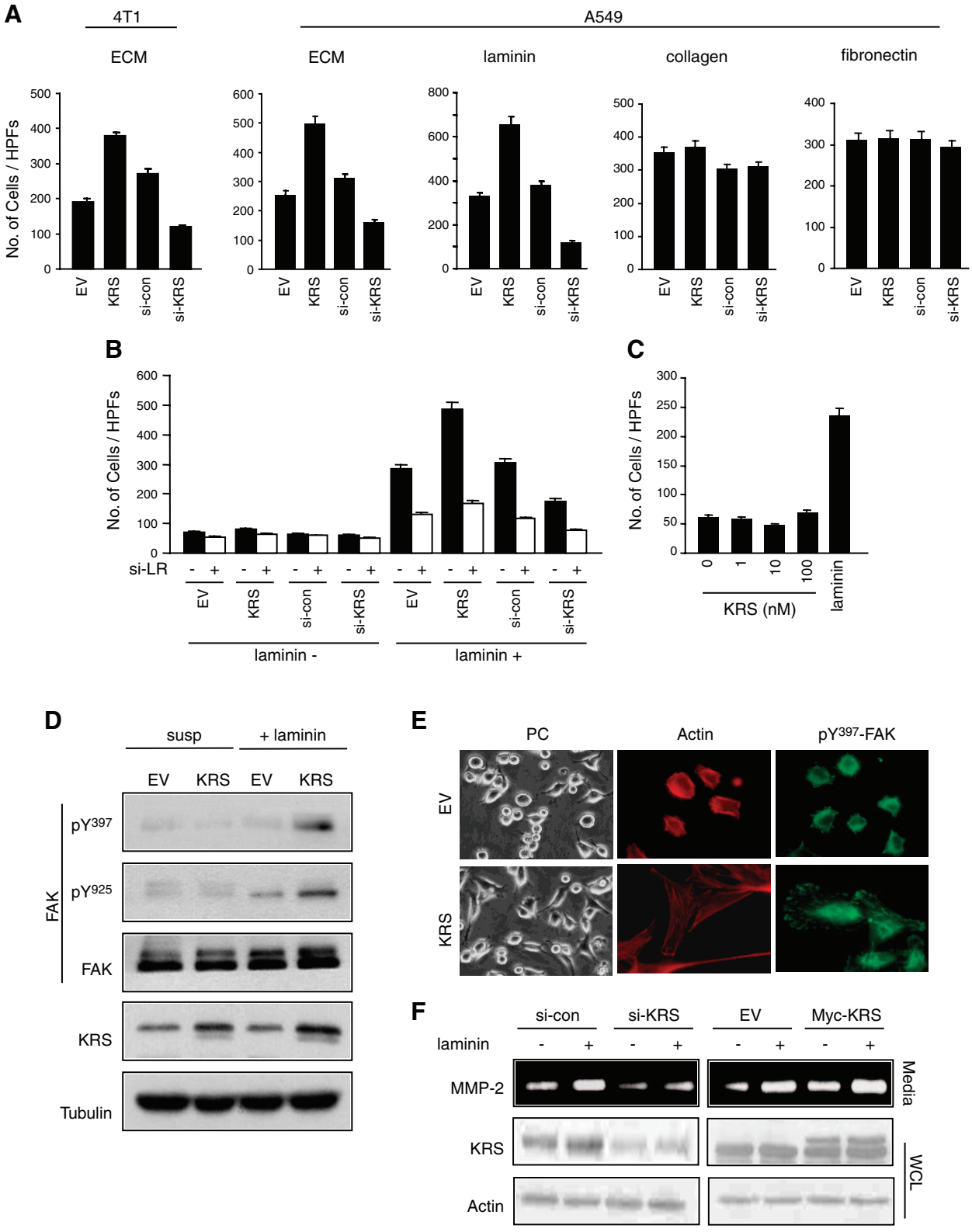

Figure 1. KRS enhances laminin-dependent cell migration. *A*) The effect of KRS on the migration of 4T1 and A549 cells in the presence of ECM or different components was determined by Transwell chamber assays. KRS expression levels were varied by transfection of Myc-KRS or its specific siRNA, the cells that migrated through the membrane were counted, and the results are presented as bar graphs. High-power field (HPF; ×400). *B*) To see whether the effect of KRS on cell migration requires laminin and LR, we monitored cell migration as above in the indicated combinations of laminin and LR using A549 cells. *C*) To see whether extracellular KRS treatment can increase cell migration, A549 cells were treated with the indicated concentrations of purified KRS, and cell migration was monitored as above. Laminin was used as a positive control. *D*) Effect of KRS on cell migration was determined by the activation of FAK. The A549 cells detached from the plates were divided into two groups. One

(*continued on next page*)

in lung cancer cells, A549 cells, and 4T1 breast cancer cells and monitored the resulting cell behavior such as proliferation, death, and migration. Surprisingly, cell migration was varied depending on the expression level of KRS in the presence of ECM (**Fig. 1*A***). To determine which component of ECM would be specifically involved in the effect of KRS on cell migration, we repeated the same experiments in the culture medium containing different components of ECM. The effect of KRS expression on cell migration was only apparent in the presence of laminin but not of collagen or fibronectin (Fig. 1*A*). In fact, the effect of KRS on cell migration was significantly reduced when the LR expression was suppressed with its specific siRNA or without laminin (Fig. 1*B*). Because KRS is secreted as a proinflammatory cytokine (13), we examined whether extracellular KRS would also affect cell migration. When A549 cells were treated with purified KRS at different concentrations, migration was not affected by extracellular treatment of KRS (Fig. 1*C*), excluding the extracellular effect of KRS on cell migration. However, changes in the KRS level had little influence on cell proliferation and death (data not shown).

Laminin induces cell migration *via* the activation of FAK (28, 29). We evaluated the effect of KRS on migration by the FAK activity (30) that is indicated by the phosphorylation of FAK at Y397 (31) and Y925 (32). The suspended EV- or KRS-transfected A549 cells in serum-free medium were divided into two groups; one group was kept in suspension culture and the other group was reseeded on the laminin-coated culture dishes. KRS significantly enhanced the FAK activity in the cells cultivated on the laminin-coated culture dishes but not in the suspension culture (Fig. 1*D*), suggesting that the effect of KRS on migration required the adhesion of the cells to the laminin-coated surface. We also monitored the effect of KRS on cell migration by cell morphology and immunofluorescence staining of actin and FAK after reseeding onto laminin-coated coverslips, which are the known signatures of cell migration. KRS overexpression changed cell morphology, distribution of actin, and the activated FAK to a more-branched and spread shape, reflecting the migratory cells (Fig. 1*E*). Because laminin treatment results in the activation of matrix metalloproteinase-2 (MMP-2; ref. 33), we checked the effect of KRS on the laminin-dependent activation of MMP-2 using zymography. The laminin-induced MMP-2 activity was ablated when KRS was suppressed with its siRNA (Fig. 1*F*, left panel) but enhanced by overexpression of KRS (Fig. 1*F*, right panel). All of these results suggest that KRS can control laminin-dependent cell migration *via* 67LR.

Specific interaction of KRS and 67LR in plasma membrane

To understand the molecular mechanism for promigratory activity of KRS, we screened cellular proteins that can bind to human KRS by yeast 2-hybrid screening using HeLa cell cDNA library. As the bait, we used the 597-aa full-length and 72-aa N-terminal eukaryote-specific extension that is thought to be involved in its interactions (34).The full-length KRS bait pulled out AIMP2/p38 (gene identification: 7965; ref. 35) that is already known to bind KRS in MSC (36) and FANCC-interacting protein (FAZF; gene identification: 27033). The N-terminal peptide of KRS selected hypoxanthine phosphoribosyltransferase 1 (HPRT1; gene identification: 3251), RPSA (also known as ribosomal subunit p40, gene identification: 3921), and cyclophilin B (cypB, gene identification: 5479) as potential KRS-binding proteins. Among them, p40 attracted our attention because p40 is also called 37LRP, which is converted to 67LR (17).

The specific interaction between the full-length KRS and 37LRP was confirmed by the yeast 2-hybrid assay. LexA-KRS generated blue colonies when paired with B42-37LRP as well as AIMP2, but not with AIMP1, another component of MSC (ref. 9 and **Fig. 2*A***). The direct interaction between KRS and the LR was tested by *in vitro* pull-down assay. GST-KRS and GST-WRS were reacted with radioactively synthesized 37LRP. 37LRP was coprecipitated with GST-KRS but not with GST-WRS (Fig. 2*B*).

We then examined whether KRS would bind either or both 37LRP and 67LR in cells. We introduced Myc-KRS into A549 cells, fractionated plasma membrane from cytoplasm, immunoprecipitated Myc-KRS from each fraction, and subjected the precipitates to immunoblotting with anti-67LR and anti-37LRP antibodies. Whereas 37LRP and 67LR were mainly detected in the cytosol and membrane fractions, respectively (Fig. 2*C*, right panel), KRS preferentially bound to 67LR in the membrane (Fig. 2*C*, left panel). To see the interaction between endogenous KRS and 67LR in A549 cells, KRS was immunoprecipitated, and coprecipitation of endogenous 67LR was determined by immunoblotting using the anti-67LR antibody specifically recognizing 67LR. 67LR was coprecipitated with KRS but not with IgG (Fig. 2*D*, top panel). Conversely, when endogenous 67LR was immunoprecipitated, KRS was specifically precipitated with 67LR but not with IgG (Fig. 2*D*, bottom panel). Interestingly, the interaction of the two endogenous proteins appeared to be increased in the presence of laminin. To further validate

group was incubated as suspension (susp) culture, and the other group was on the laminin-coated plates (+laminin). Extract from the cells was subjected to immunoblotting with the antibodies specific to p-Tyr397 and p-Tyr925 residues. Tubulin was used as a loading control. *E*) KRS- and EV-transfected A549 cells were observed for cell morphology by phase-contrast light microscopy (left) and by immunofluorescence staining with rhodamine phalloidin for actin (red, middle) and antibody against pY^{397}-FAK (green, right). *F*) The relationship of KRS to cell migration was also determined by MMP-2 activity. KRS expression in A549 cells was varied as above. MMP-2 activity and expression of KRS were quantified by zymography (top) and immunoblotting (bottom), respectively. Actin was used as a loading control. WCL, whole-cell lysate.

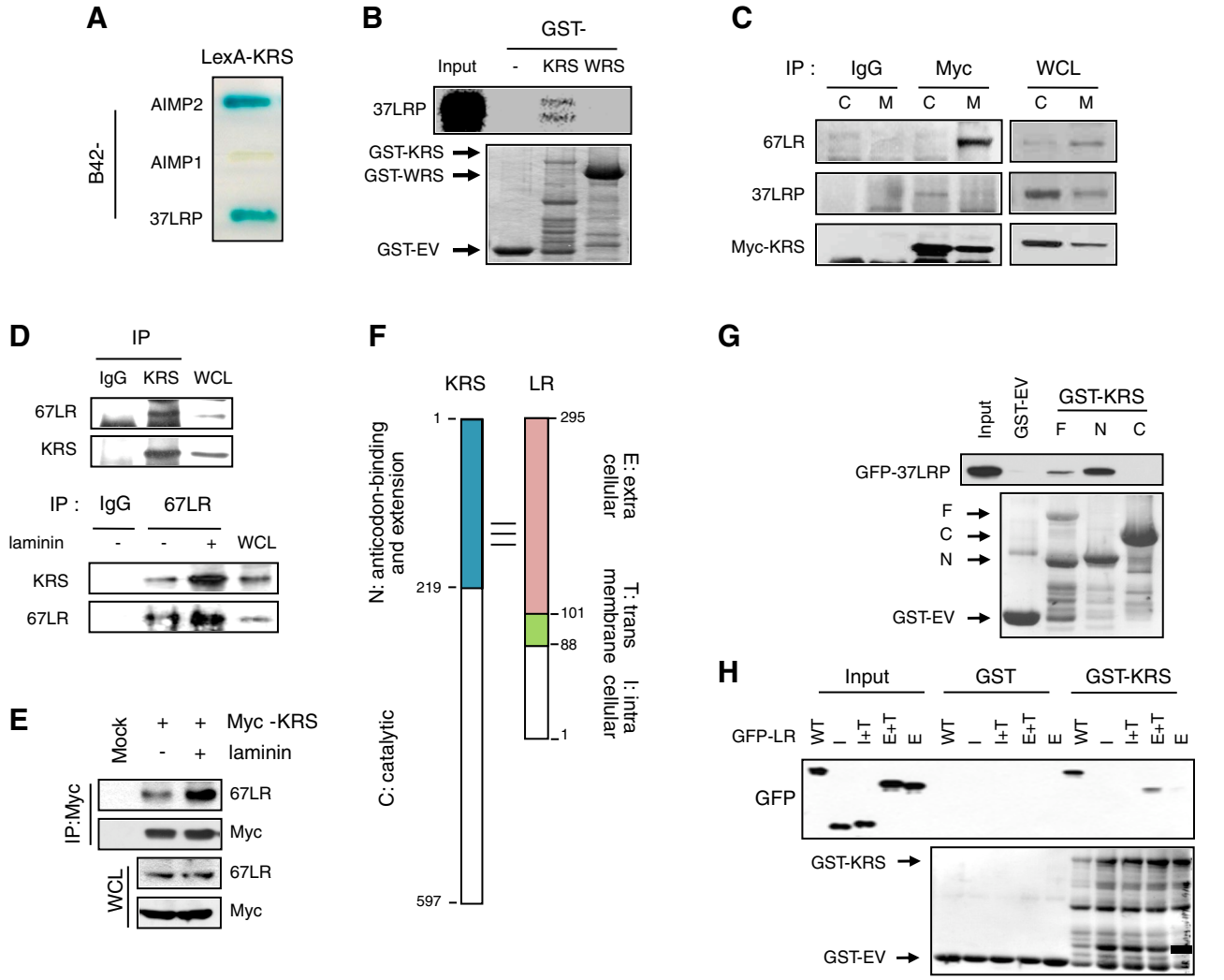

Figure 2. Interaction between KRS and LR. *A*) Interaction between full-length human KRS and 37LRP/p40 was determined by a yeast 2-hybrid assay. AIMP2 and AIMP1 were used as positive and negative controls, respectively (35). Positive interaction is indicated by blue colony formation on yeast medium containing X-gal. *B*) Top panel: 37LRP was synthesized by *in vitro* translation in the presence of [^{35}S]methionine and was subjected to pulldown with GST, GST-KRS, and GST-WRS. 37LRP coprecipitated with GST proteins was detected by autoradiography. Bottom panel: Coomassie staining of GST proteins added to radioactively synthesized 37LRP. *C*) On treatment with laminin, the A549 cells transfected with Myc-KRS were separated into cytosolic (C) and membrane (M) fractions and immunoprecipitated (IP) with anti-Myc antibody. The endogenous 37LRP and 67LR that were coprecipitated with Myc-KRS were determined by immunoblotting. IgG was used as control. *D*) Interaction of endogenous KRS with 67LR was determined by coimmunoprecipitation. Top panel: endogenous KRS was immunoprecipitated with its specific antibody, and coprecipitation of 67LR was determined by immunoblotting with the corresponding antibody (F-18; Santa Cruz Biotechnology.). Bottom panel: endogenous 67LR of A549 cells was immunoprecipitated with its specific antibody and coprecipitation of KRS was immunoblotted with anti-KRS antibody. *E*) Myc-KRS in laminin-untreated and -treated A549 cells was immunoprecipitated with anti-Myc antibody, and coprecipitated 67LR was determined by immunoblotting with anti-67LR antibody. *F*) Arrangement of functional domains in human KRS and 37LRP. Domains of KRS were divided into 219-aa N (anticodon-binding and extension domain) and 378-aa C (catalytic domain) fragments. 37LRP were separated to the indicated fragments. *G*) Top panel: GST-fused full-length (F) and N and C domains of human KRS were reacted with GFP-37LRP. They were precipitated with glutathione-Sepharose beads, and coprecipitated GFP-LR fragment was detected by immunoblotting with anti-GFP antibody. Bottom panel: Coomassie staining of GST proteins added to GFP-37LRP. *H*) GFP-fused domains of human 37LRP were reacted with GST-KRS-F. The mixture was precipitated with glutathione-Sepharose beads, and coprecipitated GFP-37LRP fragments were determined by immunoblotting with anti-GFP antibody. WCL, whole-cell lysate.

this observation, exogenously introduced Myc-KRS was precipitated from A549 cells that were cultivated in the absence and presence of laminin. The amount of 67LR coprecipitated with Myc-KRS was significantly increased in the presence of laminin (Fig. 2*E*). We determined the peptide regions of the two proteins that are involved in interaction. Human KRS was divided into the 219-aa N-terminal anticodon-binding and extension and 378-aa C-terminal catalytic domain (37), and 37LRP consists of 3 functional domains of 88 aa (1-88) intracellular, 13 aa (aa 89-101) transmembrane, and 194 aa (aa 102-295) extracellular domains (ref. 19 and Fig. 2*F*). The interaction of full-length (F), N-terminal, and C-terminal domains of GST-KRS with GFP-37LRP was tested by *in vitro* pulldown

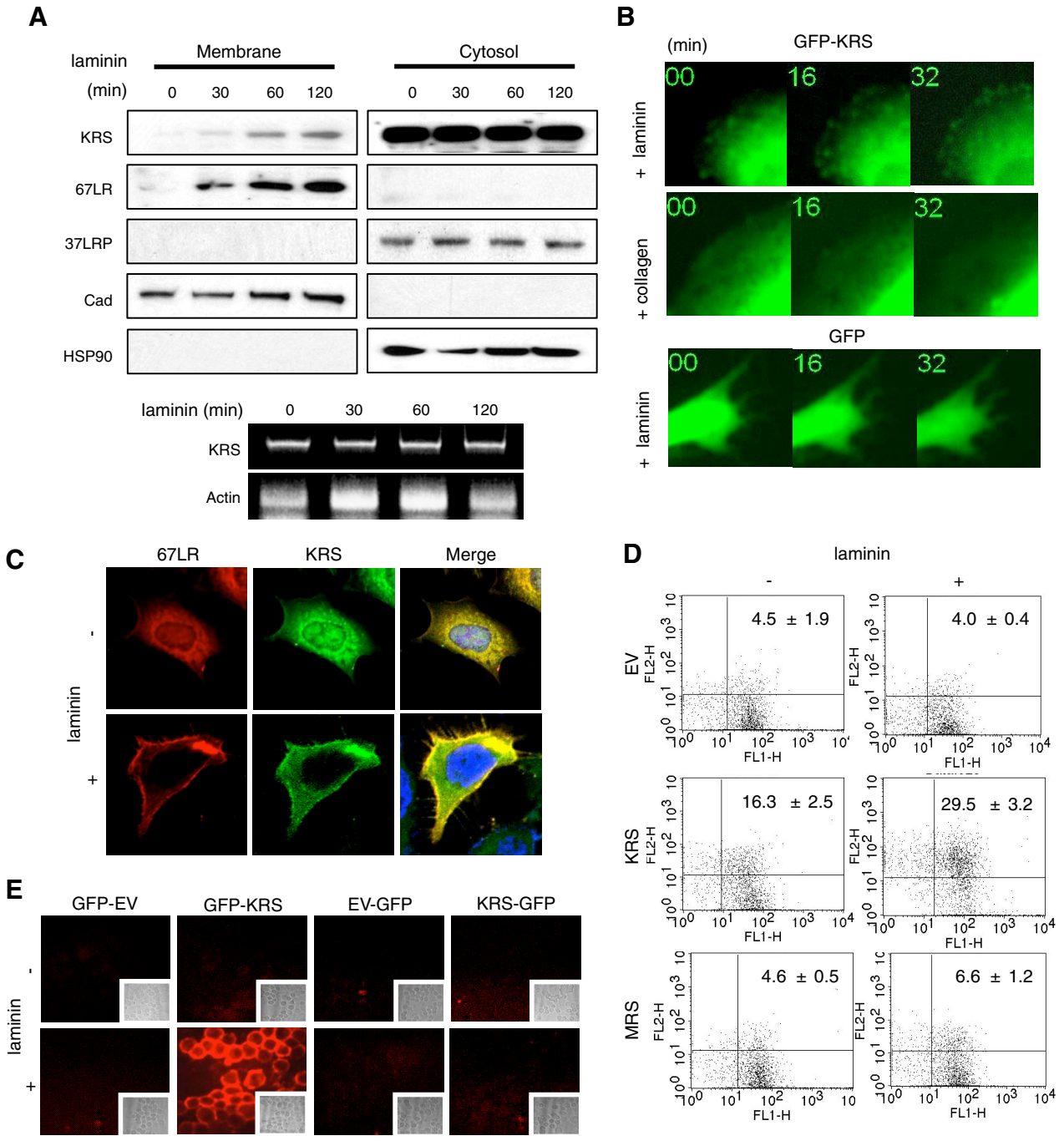

Figure 3. Laminin-induced membrane localization of KRS. *A*) A549 cells incubated in the presence of laminin (10 μg/ml) were harvested at the indicated times and separated into plasma membrane and cytosolic fractions. Top panel: levels of 67LR, 37LRP, and KRS were determined by immunoblotting. HSP90 and cadherin (Cad) were used as the markers for cytosol and membrane, respectively. Bottom panel: A549 cells were treated with laminin in a time-dependent manner, and the effect on the transcription level of KRS *via* laminin was determined by RT-PCR. Actin was used as a loading control. *B*) A549 cells transfected with GFP-KRS or GFP were treated with laminin or collagen. Cellular localization of GFP-KRS was monitored by live cell fluorescence microscopy (see Supplemental Movie S1). *C*) Cellular localization of endogenous 67LR and KRS in A549 cells in the absence and presence of laminin was determined with the antibodies conjugated with Alexa 555 (red) and 488 (green), respectively. *D*) Amounts of surface-exposed KRS and MRS were monitored by flow cytometry using anti-Myc antibodies in the laminin-untreated and -treated A549 cells transfected with Myc-KRS or Myc-MRS. *E*) GFP was attached to either the N-terminal (GFP-KRS) or C-terminal (KRS-GFP) end of KRS and expressed in A549 cells. Cells were then incubated in the absence and presence of laminin, and the extracellularly exposed GFP was monitored by immunofluorescence staining with the antibody against GFP as described in Materials and Methods. Insets: cells observed by light microscope, indicating that the cells were grown to similar confluence.

assay. GST-KRS-N as well as GST-KRS-F was coprecipitated with GFP-37LRP (Fig. 2*G*). Conversely, different domains of GFP-37LRP were subjected to affinity precipitation with GST-KRS-F. Among the LR fragments tested, extracellular and transmembrane (E+T) domains bound to KRS (Fig. 2*H*). Taken together, our results show that the N-terminal extended domain of KRS appears to interact with the C-terminal region of LR (Fig. 2*F*).

Laminin-induced translocation of KRS to plasma membrane

To see whether membrane localization of KRS is induced by laminin, we fractionated cells into cytosol and plasma membrane and determined the KRS levels by immunoblot at time interval after laminin treatment. The membrane levels of KRS were gradually increased after laminin treatment although the majority of KRS still remained in cytosol (**Fig. 3*A***, top panel). Under the same conditions, KRS expression was not changed as determined by RT-PCR (Fig. 3*A*, bottom panel). To see the effect of laminin on KRS localization in live cells, we expressed GFP-KRS in A549 cells treated with laminin or collagen and monitored the change in KRS localization by fluorescence microscopy. When the cells were treated with laminin, dynamic foci formation of GFP-KRS, but not of GFP alone, was observed in the plasma membrane although the majority of KRS still remained in cytosol (Fig. 3*B*, top and bottom panels, and Supplemental Movie S1). The membrane foci of GFP-KRS were not observed when the cells were treated with collagen (Fig. 3*B*, middle panel, and Supplemental Movie S1). Laminin-induced membrane enrichment of endogenous KRS was also observed by immunofluorescence microscopy (Fig. 3*C*).

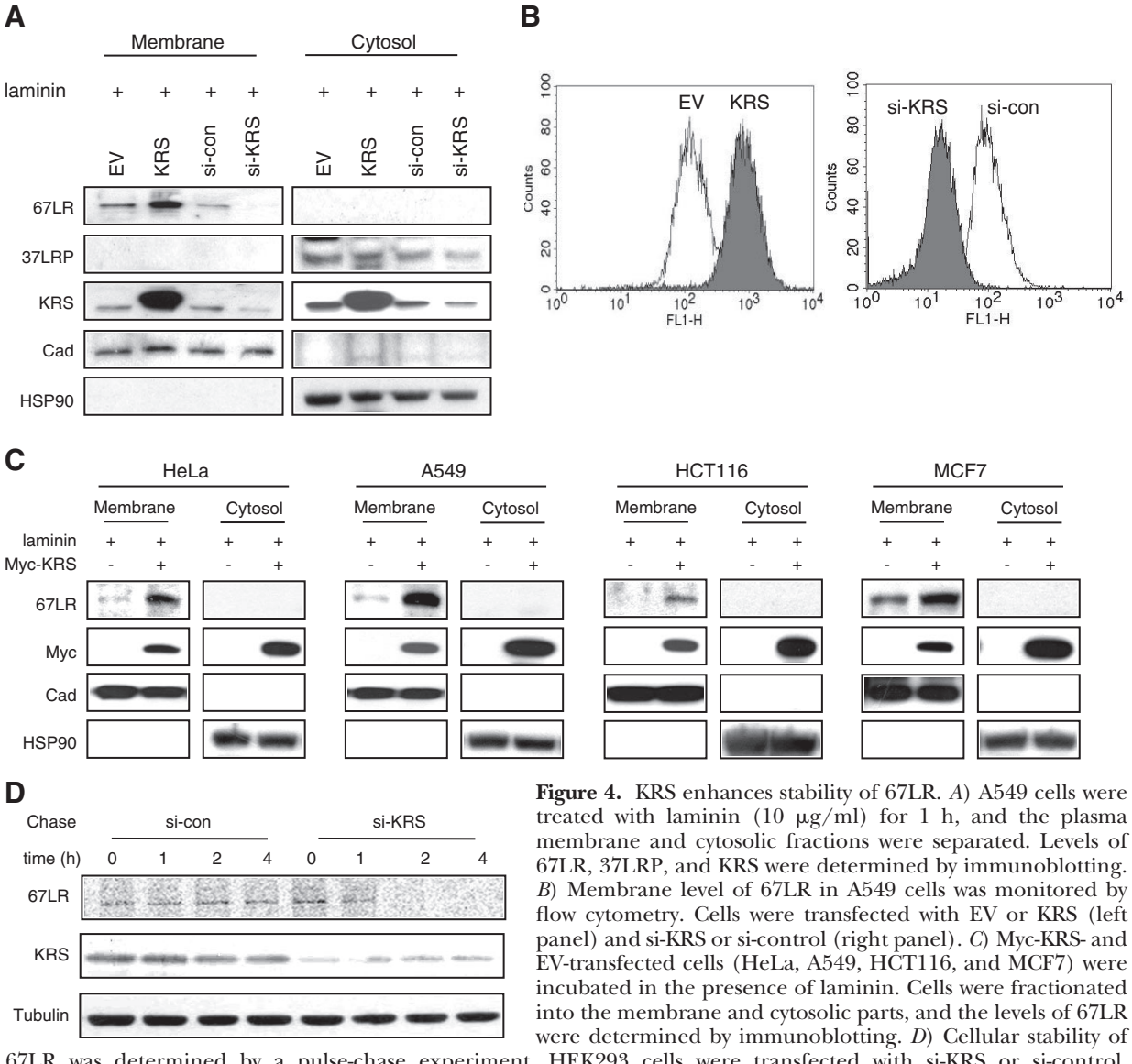

Figure 4. KRS enhances stability of 67LR. *A*) A549 cells were treated with laminin (10 μg/ml) for 1 h, and the plasma membrane and cytosolic fractions were separated. Levels of 67LR, 37LRP, and KRS were determined by immunoblotting. *B*) Membrane level of 67LR in A549 cells was monitored by flow cytometry. Cells were transfected with EV or KRS (left panel) and si-KRS or si-control (right panel). *C*) Myc-KRS- and EV-transfected cells (HeLa, A549, HCT116, and MCF7) were incubated in the presence of laminin. Cells were fractionated into the membrane and cytosolic parts, and the levels of 67LR were determined by immunoblotting. *D*) Cellular stability of 67LR was determined by a pulse-chase experiment. HEK293 cells were transfected with si-KRS or si-control. [^{35}S]methionine was incorporated for 1 h. 67LR was immunoprecipitated with anti-67LR antibody, separated by SDS-PAGE, and autoradiographed. Suppression of KRS with its specific siRNA was confirmed by immunoblotting. Cad, cadherin.

We examined the surface exposure of KRS in A549 cells by flow cytometry with anti-Myc antibody after transfection with Myc-KRS. The amount of exposed KRS was enhanced approximately 2-fold by laminin treatment (Fig. 3*D*, middle panel). In contrast, the signal was not much changed in the cells that were transfected with EV or Myc-MRS regardless of laminin treatment (Fig. 3*D*, top and bottom panels). This result suggests that the laminin-dependent surface exposure is specific to KRS. To determine which side of KRS is exposed out of the cells, we fused GFP tag to the N- or C-terminal end of KRS and introduced it into A549 cells. We incubated the transfected cells in the presence and absence of laminin, labeled unpermeabilized cells with QD625-conjugated to anti-GFP antibody, and visualized by fluorescence. GFP fused to the N-terminal end of KRS gave fluorescence from the laminin-treated cells (Fig. 3*E*), suggesting that the N-terminal end of KRS should be exposed from the cell membrane.

KRS enhances membrane stability of 67LR

To understand the functional implication for the interaction of KRS with 67LR in membrane, we separated cells into plasma membrane and cytosol and examined the changes in 67LR levels in each fraction by various KRS levels. The 67LR level in the plasma membrane was enhanced by the increase in KRS but was reduced when KRS was suppressed with its siRNA (**Fig. 4*A***). The positive effect of KRS on the 67LR membrane level was also observed by flow cytometry (Fig. 4*B*). KRS also increased the membrane levels of 67LR in different cancer cell types (Fig. 4*C*), suggesting that the functional connection of KRS with 67LR in cell migration could be applicable to many different cancer cells.

We investigated how KRS enhances the membrane level of 67LR. We changed the expression level of KRS by ectopic expression or knockdown of KRS in A549 cells and the effect of KRS on the mRNA level of 37LRP was determined by semiquantitative RT-PCR. The mRNA level of 37LRP was not affected by the changes in KRS expression (Supplemental Fig. S1*A*). We also examined whether KRS would mediate fatty acylation of 37LRP, known to be required for the conversion of 37LRP to 67LR (38, 39). The acylation of 37LRP was not significantly influenced by the various KRS expression (Supplemental Fig. S1*B*). We also checked the effect of KRS on turnover of 67LR by a pulse-chase experiment. Nascent protein synthesis was labeled with radioactive methionine. Disappearance of 67LR was monitored by autoradiography at time intervals. 67LR was more rapidly decreased when KRS was suppressed with its siRNA (Fig. 4*D*). Thus, KRS appears to extend the half-life of 67LR in the plasma membrane through its association with 67LR. Because integrins are the major receptor family of laminin (40), we tested whether KRS can also affect the membrane levels of different integrins by flow cytometry. None of the tested integrins was influenced by the overexpression of KRS (Supplemental Fig. S1*C*), suggesting that the effect of KRS is specific to 67LR.

Because KRS can be secreted in some cancer cells (13), we tested whether KRS secretion can be induced by laminin treatment in A549 cells and found no apparent secretion (Supplemental Fig. S2). To see whether extracellular KRS could affect membrane localization of 67LR, we treated A549 cells with purified recombinant KRS and laminin and compared the membrane levels of 67LR. The 67LR level was increased by laminin but not by KRS treatment (Supplemental Fig. S3*A*). We also compared the effect of intra- and extracellular KRS on the membrane levels of 67LR and found that the 67LR level was significantly enhanced by ectopic expression of KRS but not by the extracellular treatment of recombinant KRS (Supplemental Fig. S3*B*).

Laminin-induced phosphorylation of KRS is involved in membrane localization

Cytosolic KRS is mainly bound to MSC. To see whether the membrane translocation of KRS involves its dissociation from MSC, we immunoprecipitated MSC from the laminin-untreated and -treated A549 cells using the antibody against glutamyl-prolyl-tRNA synthetase (EPRS), another component of MSC, and determined whether the amount of KRS bound to MSC is reduced by laminin treatment. The amount of KRS coprecipitated with EPRS was decreased by laminin treatment (**Fig. 5*A***, left panel), whereas the portion of KRS dissociated from MSC was increased in the immuno-depleted fraction (Fig. 5*A*, right panel), suggesting that KRS located in the plasma membrane should be originated from MSC.

KRS was previously known to be translocated into nucleus *via* phosphorylation (12). We examined whether phosphorylation is also involved in the laminin-induced membrane translocation of KRS. We mixed the purified GST-KRS with the protein extracts from the laminin-untreated and -treated A549 cells in the presence of [γ-^{32}P]ATP, and the reaction mixtures were subjected to autoradiography. Radioactivity of GST-KRS was detected by the incubation of the extract and significantly increased by the incubation of laminin-treated cells (Fig. 5*B*). No radioactivity was observed when GST was reacted with either of the extracts. Because laminin treatment activates PI3K (41, 42), we determined whether PI3K is involved in the phosphorylation of KRS. Phosphorylation of GST-KRS was performed as above with the protein extracts from A549 cells with and without the treatment with LY294002, the PI3K inhibitor. Laminin-induced phosphorylation of KRS was inhibited when the cells were treated with LY294002 (Fig. 5*C*), suggesting that KRS phosphorylation would involve PI3K. To determine the downstream kinase that can be responsible for the laminin-induced phosphorylation of KRS, we introduced each of 3 different MAPKs, and interaction with KRS was determined by coimmunoprecipitation. Among the three kinases, p38MAPK was coimmunoprecipitated with Myc-KRS when laminin is treated (Fig. 5*D*). The interaction between Myc-KRS and p38MAPK was significantly increased by laminin treatment (Fig. 5*E*), and it was further confirmed by coimmunoprecipitation between the

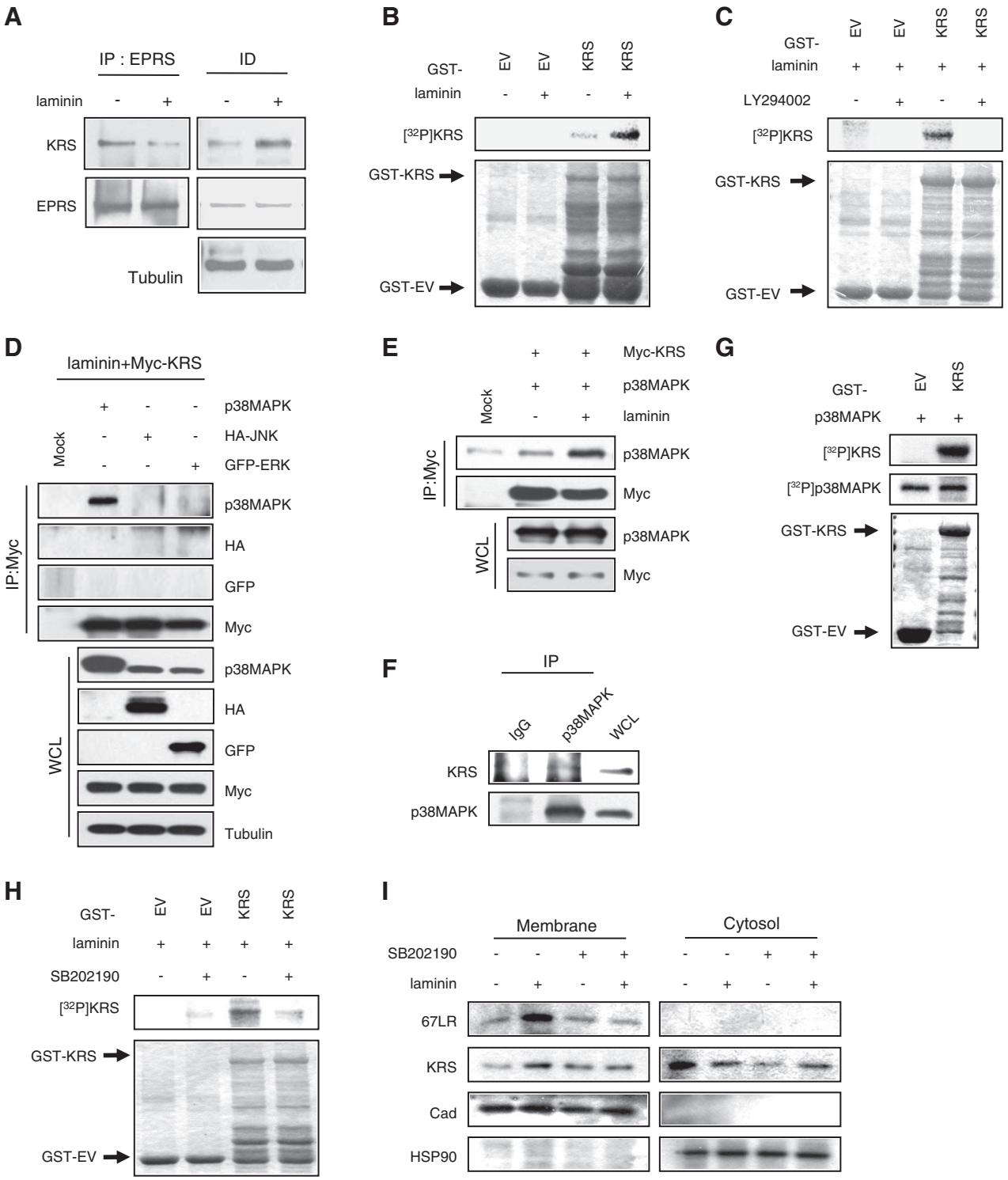

Figure 5. p38MAPK-mediated phosphorylation is required for laminin-induced dissociation of KRS from the multisynthetase complex. *A*) Extracts from A549 cells that were cultivated in the absence and presence of laminin were immunoprecipitated with antibody against EPRS, one of the enzyme components for MSC. The mixture was separated into immunoprecipitate (IP) and the immunodepleted supernatant (ID), and each fraction was subjected to immunoblotting with anti-KRS and anti-EPRS antibodies. *B*) GST and GST-KRS were purified and reacted with the protein extracts from A549 cells incubated in the absence and presence of laminin in the presence of [γ-^{32}P]ATP. Radioactivity of GST-KRS was determined by autoradiography. *C*) Kinase assay was conducted as above in the absence and presence of LY294002. *D*) KRS binding to three different MAPKs (p38MAPK, JNK, and ERK) was tested by coimmunoprecipitation. p38MAPK, HA-JNK, and GFP-ERK were transfected into A549 cells with Myc-KRS, and the cells were treated with laminin. KRS was immunoprecipitated with anti-Myc antibody, and coprecipitation of different MAPKs was determined by immunoblotting with their respective antibodies. *E*) Myc-KRS and p38MAPK were expressed in A549 cells that were incubated in the absence and presence of laminin. KRS was immunoprecipitated with anti-Myc antibody,

(*continued on next page*)

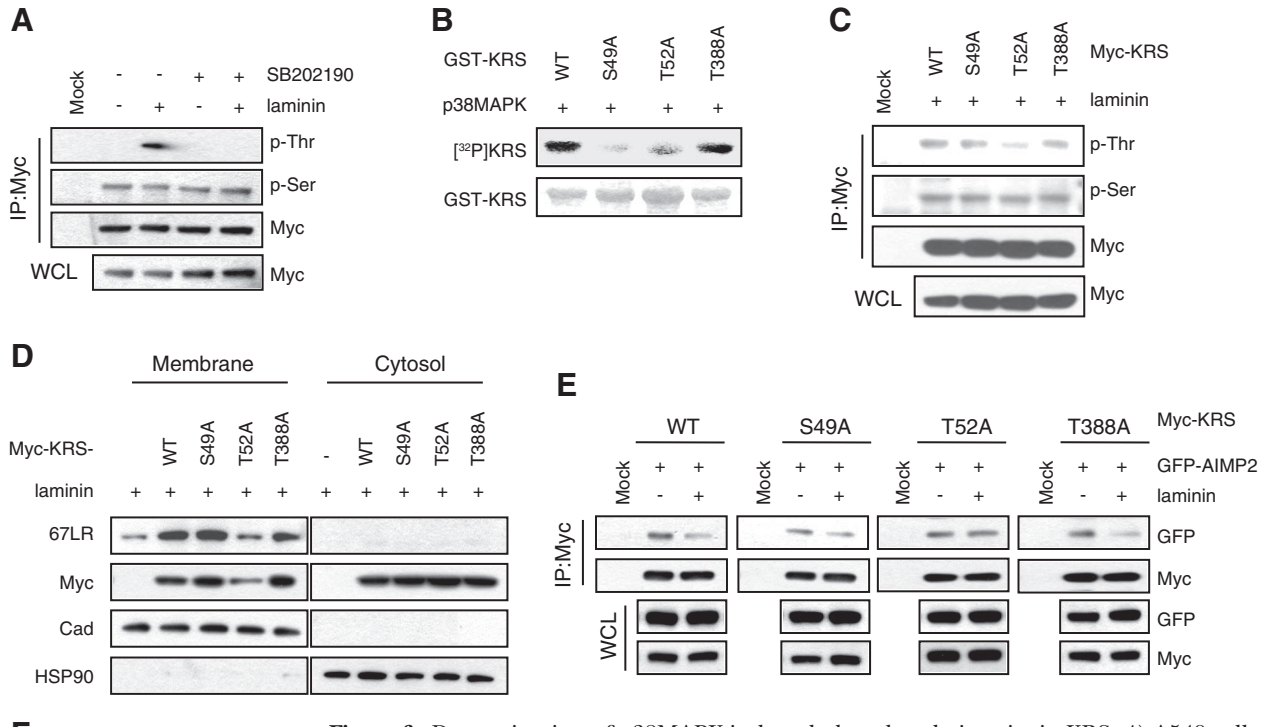

Figure 6. Determination of p38MAPK-induced phosphorylation site in KRS. *A*) A549 cells expressing Myc-KRS were incubated in different combinations of SB202190 and laminin. Myc-KRS was immunoprecipitated (IP) and phosphorylation at threonine and serine was determined by anti-p-Thr and anti-p-Ser antibodies. *B*) GST-KRS proteins containing S49A, T52A, and T388A mutations were reacted with p38MAPK in the presence of [γ-^{32}P]ATP, and phosphorylation was determined by autoradiography. *C*) Each Myc-KRS mutant was expressed in A549 cells and incubated in the presence of laminin. Myc-KRS was immunoprecipitated and subjected to immunoblotting with anti-p-Thr and anti-p-Ser antibodies. *D*) Same cells as above were fractionated into plasma membrane and cytosol, and the amounts of 67LR and KRS were determined by immunoblotting. *E*) GFP-AIMP2 and each of KRS mutants were expressed in A549 cells in the presence and absence of laminin. Myc-KRS was immunoprecipitated, and coprecipitation of GFP-AIMP2 was determined by immunoblotting. *F*) Effect of KRS mutant on migration *via* laminin was determined by using Transwell chamber assays. A549 cells were transfected with each of KRS mutants. Cells that migrated through the membrane were counted, and the results are presented as bar graphs. Cad, cadherin; WCL, whole-cell lysate; HPF, high-power field.

endogenous KRS and p38MAPK (Fig. 5*F*). To see whether p38MAPK can actually phosphorylate KRS, we incubated GST or GST-KRS with purified p38MAPK as above. GST-KRS, but not GST, was indeed phosphorylated by p38MAPK (Fig. 5*G*). We determined whether p38MAPK is actually necessary for laminin-induced phosphorylation of KRS using its inhibitor, SB202190. The laminin-induced phosphorylation of GST-KRS was inhibited when the cells were treated with SB202190 (Fig. 5*H*), indicating the functional relevance of p38MAPK for KRS phosphorylation. The treatment of A549 cells with SB202190 inhibited translocation of KRS to membrane and also ablated laminin-dependent increase of 67LR in the membrane (Fig. 5*I*). All of these results suggest that laminin induces phosphorylation of KRS through the PI3K and p38MAPK pathway, and this process is required for membrane localization of KRS and its effect on 67LR.

Determination of laminin-induced phosphorylation site in KRS

To determine the laminin-induced phosphorylation site in KRS, we incubated Myc-KRS transfected A549 cells in the different combination of SB202190 and laminin. The immunoprecipitated Myc-KRS was sub-

and coprecipitation of p38MAPK was determined by immunoblotting. *F*) Interaction of endogenous p38MAPK and KRS was also determined by coimmunoprecipitation. p38MAPK was immunoprecipitated with its specific antibody from A549 cells, and coprecipitation of KRS was determined by immunoblotting. *G*) GST or GST-KRS was reacted with purified p38MAPK in the presence of [γ-^{32}P]ATP, and phosphorylation was determined by autoradiography. The activity of p38MAPK was confirmed by autophosphorylation. *H*) Purified GST and GST-KRS were reacted with the protein extracts from A549 cells that were incubated in the presence of laminin with and without SB202190. The radioactivity of GST-KRS was determined as above. *I*) A549 cells incubated in the combination of SB202190 and laminin were fractionated into plasma membrane and cytosol, and the amounts of 67LR and KRS in each fraction were determined by immunoblotting. Cad, cadherin; WCL, whole-cell lysate.

jected to immunoblot with anti-p-Thr and anti-p-Ser antibodies. The p-Thr signal was enhanced by laminin treatment but blocked with SB202190, whereas the p-Ser signal was not changed (**Fig. 6*A***). To determine the phosphorylation site, we reacted the GST-KRS with p38MAPK and subjected the reaction mixture to mass analysis. Two phosphopeptides, QLSQATAAATNHTTDNGVGPEEESVDPNQYYK and VTYHPDGPEGQAYDVDFTPPFR, were identified. Among these two peptides, S49, T52, and T388 residues were predicted to be the potential phosphorylation sites by p38MAPK. To validate whether any of these sites is actually phosphorylated by p38MAPK, these sites were mutated to alanine, and each of the GST-KRS mutants was subjected to *in vitro* kinase assay as above. The radioactivity of KRS was significantly reduced by the S49A or T52A mutant (Fig. 6*B*). To further validate the effect of these mutations, Myc-KRS mutant-introduced A549 cells were incubated in the presence of laminin. Phosphorylation of immunoprecipitated KRS was determined by immunoblotting with anti-p-Thr and anti-p-Ser antibodies. Only T52A showed significantly reduced phosphorylation (Fig. 6*C*). We then fractionated membrane from laminin-treated A549 cells and compared the membrane levels of 67LR and KRS mutants. Among the three mutants, only the T52A mutant was not translocated to membrane and also did not enhance the 67LR membrane level (Fig. 6*D*). We introduced each of the mutants into A549 cells with GFP-AIMP2 and compared whether their association with AIMP2 would be affected by laminin. Among the three mutants, binding of the T52A to AIMP2 was not affected by laminin treatment, whereas the two other mutants as well as the WT KRS dissociated from AIMP2 with laminin treatment (Fig. 6*E*). In the Transwell chamber assay, the T52A mutant lost the ability to induce cell migration, unlike the two other mutants (Fig. 6*F*).

We also made the T52D mutant that can mimic the phosphorylation of KRS and compared the T52D and T52A mutants with the WT KRS for laminin-dependent membrane localization and effect on the membrane level of 67LR. Each of the GFP-KRS WT and mutants was expressed in A549 cells, and the effect of laminin on the membrane localization was monitored by fluorescence microscopy. The T52D mutant

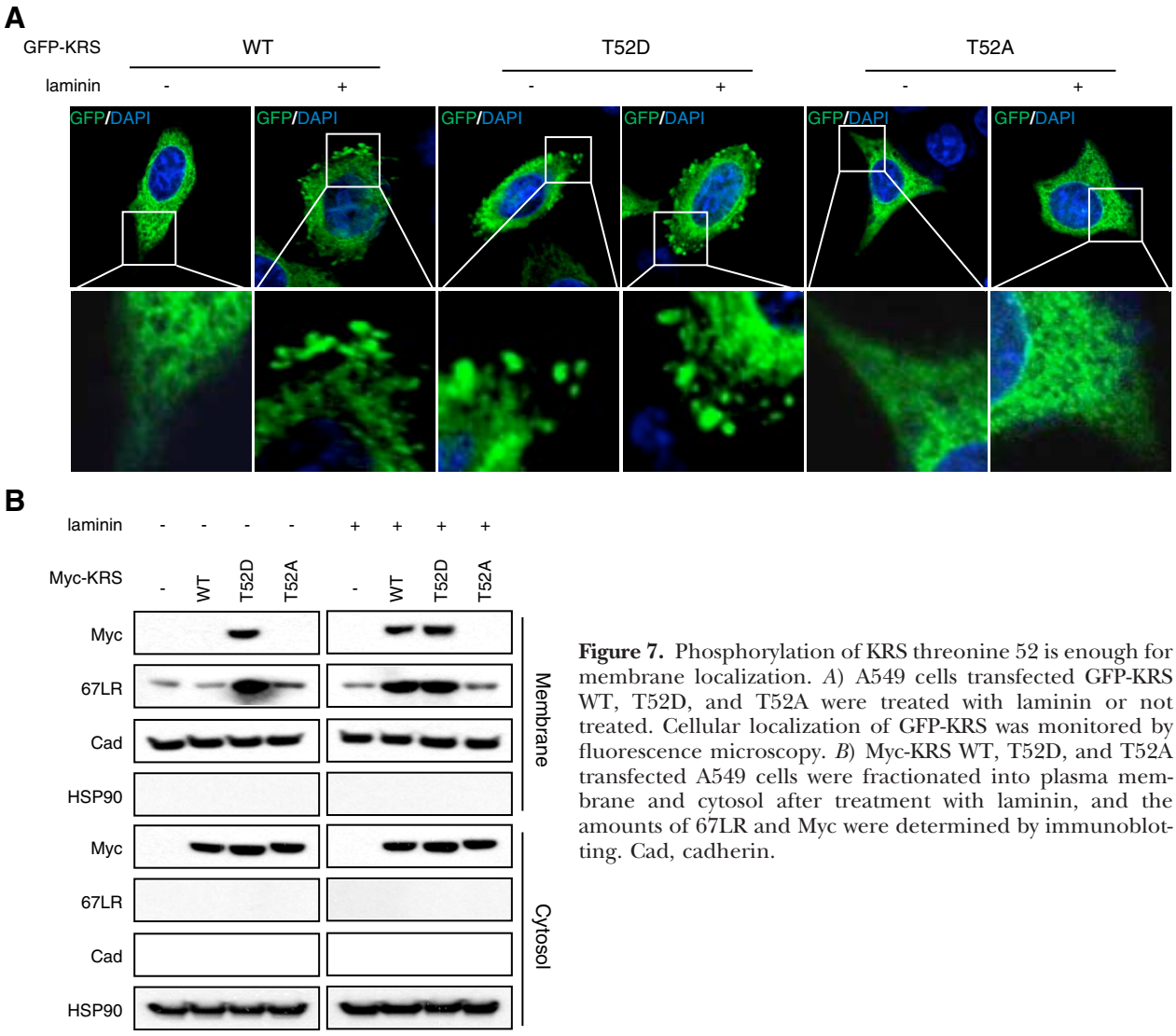

Figure 7. Phosphorylation of KRS threonine 52 is enough for membrane localization. *A*) A549 cells transfected GFP-KRS WT, T52D, and T52A were treated with laminin or not treated. Cellular localization of GFP-KRS was monitored by fluorescence microscopy. *B*) Myc-KRS WT, T52D, and T52A transfected A549 cells were fractionated into plasma membrane and cytosol after treatment with laminin, and the amounts of 67LR and Myc were determined by immunoblotting. Cad, cadherin.

showed constitutively increased membrane localization independent of laminin, whereas the membrane localization of the T52A mutant was not apparently observed (**Fig. 7*A***). Consistently, the higher level of 67LR was detected in the membrane of the T52D mutant-transfected cells regardless of laminin. In contrast, the T52A mutant was not found in the membrane and also did not increase the membrane level of 67LR (Fig. 7*B*). Taken together, these results show that T52 appears to be the site that determines cellular localization of KRS in response to laminin stimulus.

KRS inhibits ubiquitin-mediated degradation of 67LR by Nedd4

To understand how KRS would stabilize 67LR in the membrane, we investigated whether 67LR is subject to the ubiquitin-mediated degradation system. For this, we treated A549 cells with MG132, an 26S proteasome inhibitor, and determined whether the membrane level of 67LR could be stabilized. The MG132 treatment alone without laminin treatment increased the membrane level of 67LR compared with that in the control (**Fig. 8*A***). 67LR was previously reported to be enriched in membrane lipid raft (43), and Nedd4 was suggested as one of the E3 ligases that can ubiquitinate the target proteins in the lipid raft (44). We thus tested whether Nedd4 can control the 67LR membrane level. Ectopic expression of Nedd4 significantly reduced the 67LR membrane level in A549 cells, whereas suppression of Nedd4 with its short hairpin RNA increased 67LR (Fig. 8*B*). The interaction between endogenous 67LR and Nedd4 was induced by laminin treatment (Fig. 8*C*). The ubiquitinated 67LR was increased by exogenous supplementation of Nedd4 WT but not by the C894A inactive mutant (ref. 45 and Fig. 8*D*). When the effects of Nedd4 WT and C894A on the membrane level of 67LR were compared, the WT Nedd4, but not the

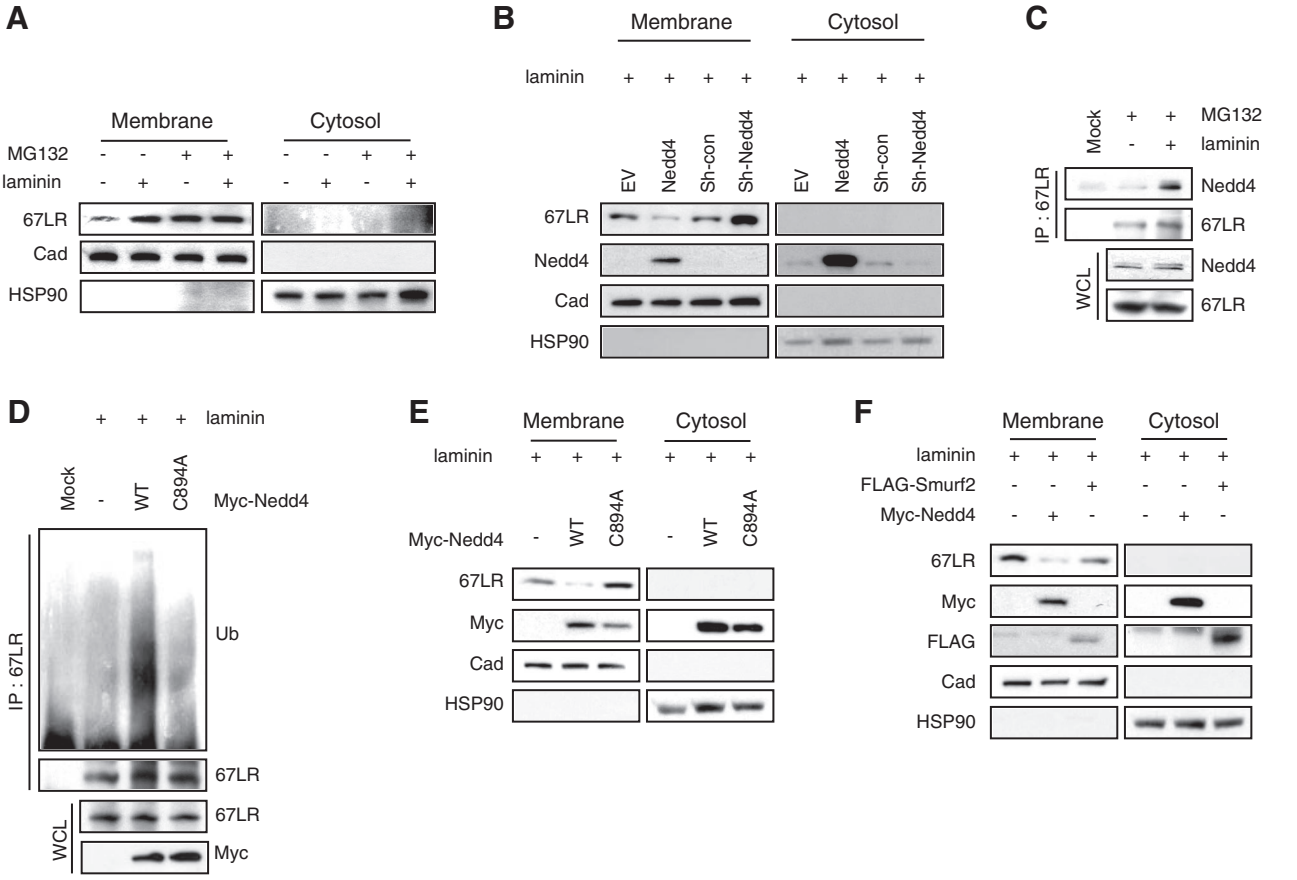

Figure 8. Nedd4 is the specific E3 ligase of 67LR. *A*) Laminin-untreated and -treated A549 cells were preincubated in the absence and presence of MG132 (50 μM, 4 h) and fractionated. Extracts from the two fractions were subjected to immunoblotting. *B*) Nedd4 was increased and decreased by transfection with Nedd4 and short hairpin (sh)-Nedd4, respectively. Transfected A549 cells were treated with laminin and fractionated into plasma membrane and cytosol. 67LR and Nedd4 were detected by immunoblotting. *C*) A549 cells preincubated with MG132 were treated with laminin or not treated. The endogenous 67LR was immunoprecipitated (IP) with anti-67LR antibody. Coprecipitates were detected by antibody against Nedd4. *D*) A549 cells transfected with Myc-Nedd4 WT or Myc-Nedd4 C894A were treated with laminin and MG132. Lysate from A549 cells was immunoprecipitated with anti-67LR antibody. Precipitates were subjected to SDS-PAGE. *E*) Same cells as above were fractionated into cytosol and membrane. *F*) A549 cells transfected with Myc-Nedd4 or FLAG-Smurf2 were treated with laminin and fractionated into cytosol and membrane. FLAG-Smurf2 was detected with anti-FLAG antibody. Cad, cadherin; WCL, whole-cell lysate.

mutant, reduced the 67LR level (Fig. 8*E*). Nedd4 is one of the HECT type E3 ligases (46). To check the specificity of Nedd4 to degradation of 67LR, we tested another HECT type E3 ligase, Smurf2 (46), to see whether it can also decrease 67LR in the membrane. The effect of Smurf2 on the 67LR membrane level was not apparently as strong as that of Nedd4 (Fig. 8*F*), suggesting that the membrane stability of 67LR is mainly controlled by Nedd4.

We then examined how KRS would affect Nedd4-mediated ubiquitination of 67LR. Laminin-induced ubiquitination of 67LR was reduced by the exogenous introduction of Myc-KRS and increased when KRS was suppressed with its siRNA (**Fig. 9*A***). Exogenous introduction of Nedd4 enhanced ubiquitination of 67LR but addition of KRS reduced Nedd4-induced ubiquitination of 67LR (Fig. 9*B*). The binding of Nedd4 to LR was also suppressed by the ectopic expression of KRS (Fig. 9*C*). The exogenous supplementation of Nedd4 significantly reduced membrane level of 67LR, but simultaneous introduction of KRS inhibited the membrane localization of Nedd4 and restored the membrane level of 67LR (Fig. 9*D*). The amount of Nedd4 in membrane was inhibited by the introduction of WT or T52D KRS, but not by T52A KRS (Fig. 9*D*). All of these results suggest that the binding of KRS to 67LR in plasma membrane is important for the protection of 67LR from the Nedd4-mediated degradation. We then examined whether laminin would trigger the binding of KRS and Nedd4 to 67LR simultaneously or sequentially. When we monitored the time course for the binding of KRS and Nedd4 to 67LR after the treatment of laminin to A549 cells, we found that KRS bound first to 67LR, followed by Nedd4 (Fig. 9*E*). This result suggests that KRS would be recruited to 67LR at the initial stage of the laminin signal to sustain the cell migration. Meanwhile, Nedd4 is induced and attracted to 67LR as negative feedback.

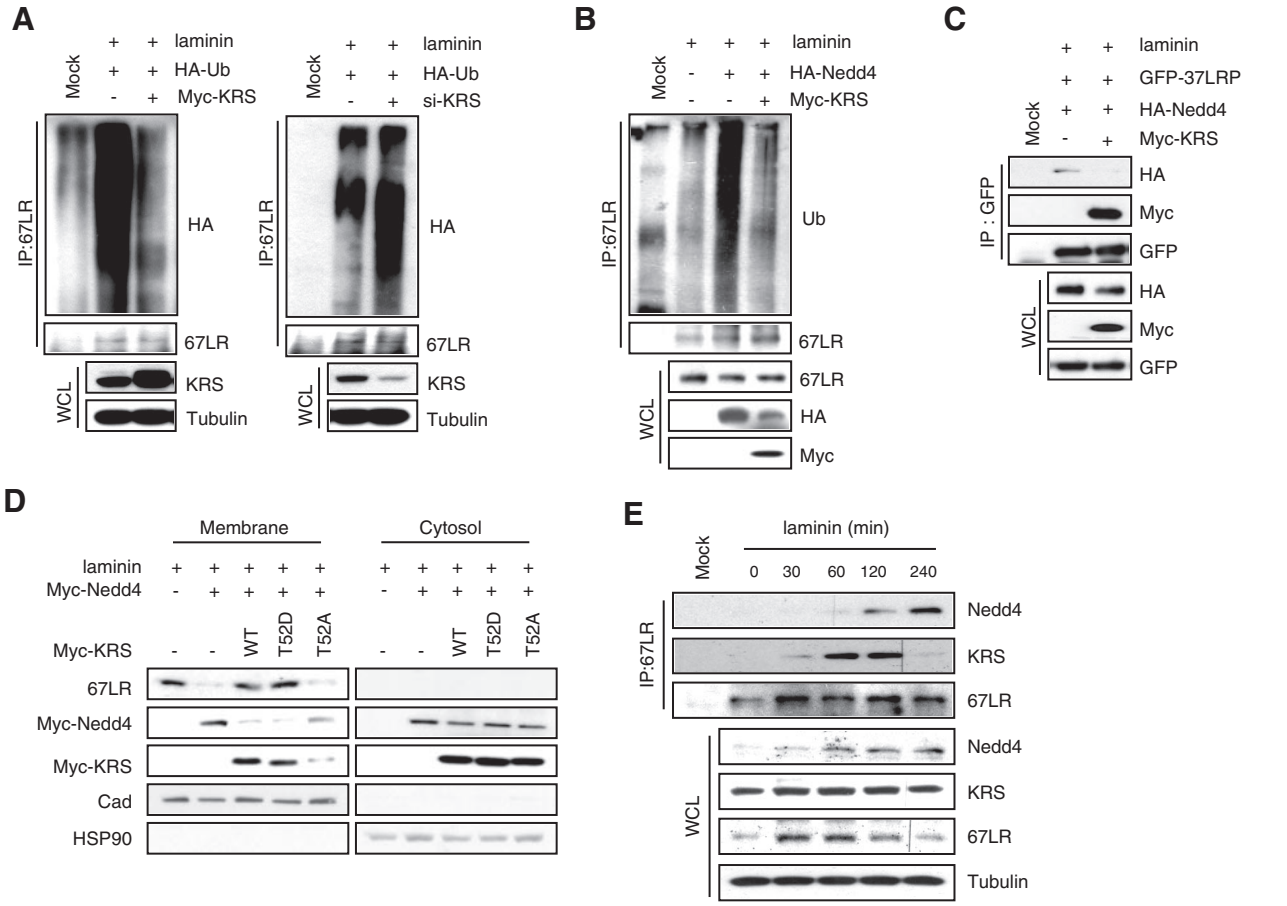

Figure 9. KRS inhibits Nedd4-mediated ubiquitination of 67LR. *A*) A549 cells transfected with HA-ubiquitin (Ub) were incubated in the presence of laminin, and KRS expression was increased and suppressed by introduction of KRS and si-KRS, respectively. Extracts from each of the transfectants were precipitated with anti-67LR antibody, and the precipitates were separated by SDS-PAGE and subjected to immunoblotting with anti-HA antibody. *B*) A549 cells transfected with the combination of HA-Nedd4 and Myc-KRS were lysed and immunoprecipitated (IP) with anti-67LR antibody. The precipitates were subjected to SDS-PAGE and immunoblotting with anti-Ub antibody. *C*) A549 cells transfected with HA-Nedd4, GFP-37LRP, and Myc-KRS were lysed and immunoprecipitated with anti-GFP antibody. Precipitates were separated by SDS-PAGE and subjected to immunoblotting. *D*) A549 cells were transfected with the indicated pairs of Myc-Nedd4 and Myc-KRS T52 mutants. The transfected cells were separated into plasma membrane and cytosolic fractions. *E*) Time course for the interaction of 67LR with KRS and Nedd4 after laminin treatment. 67LR was immunoprecipitated, and coprecipitated KRS and Nedd4 were determined by their corresponding antibodies. WCL, whole-cell lysate; Cad, cadherin.

Taken together, our results show that KRS mainly bound to MSC is phosphorylated at T52 by the PI3K-p38MAPK pathway that is activated by laminin. The phosphorylated KRS is then dissociated from MSC and translocated to plasma membrane. In the membrane, KRS binds 67LR to inhibit ubiquitination of 67LR that is mediated by Nedd4. The stabilized 67LR can mediate cell migration in a laminin-dependent manner (**Fig. 10**).

DISCUSSION

Here we identified the membrane translocation and functional interaction of the two translational components in the plasma membrane: KRS, an enzyme for protein synthesis, and LR, whose precursor is a ribosomal subunit, p40, to induce laminin-dependent cell migration. Although we conducted most of the experiments in cancer cell lines, we also found that the laminin-induced membrane translocation of KRS and its positive effect on 67LR and cell migration were also confirmed in normal lung cells WI-26 (data not shown), suggesting that the functional relationship between these two translational factors for cell migration should be generally applied. Perhaps in normal cells, the membrane translocation of KRS could be tightly controlled, but it could be out of control in cancer cells if KRS is either overexpressed or mutated. In this regard, it is worth noting that KRS is often highly expressed in cancer cells (13, 47–49). It is not yet clear why the cells recruit translational components to plasma membrane to control cell migration. One possibility is that the membrane localization of these factors may reduce the levels of operational translational machinery. KRS also plays a key role in the structural stability of the multisynthetase complex (9). Thus, dissociation of KRS may also affect the cellular levels of other synthetase components within the complex although it is to be determined how much these changes would affect global translation.

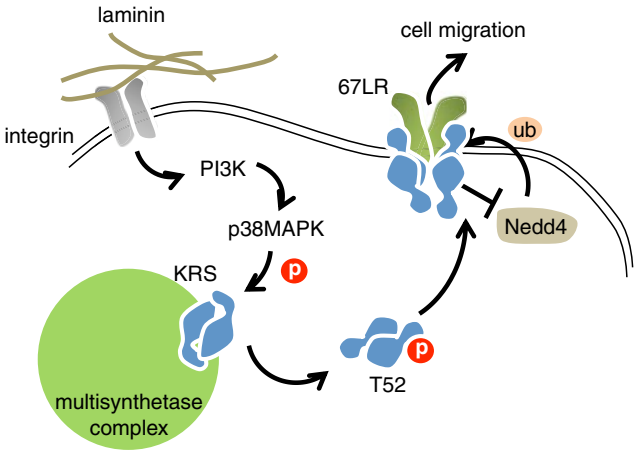

Figure 10. Proposed model for cell migration control of KRS *via* 67LR in plasma membrane. Laminin binding to integrin can activate PI3K and its downstream p38MAPK, which then introduces phosphorylation at the T52 residue of KRS that is normally bound to MSC. The phosphorylated KRS dissociates from MSC and is mobilized to plasma membrane. In the membrane, it binds to 67LR, preventing Nedd4-mediated ubiquitination to 67LR to extend the membrane stability of 67LR. Thus, KRS binding to 67LR can enhance laminin-induced cell migration. The laminin signal can be also introduced *via* the preexisting 67LR and the membrane trafficking of KRS can work as a positive feedback mechanism. ub, ubiquitin.

Although 37LRP showed the potential for the interaction with KRS (Fig. 2*A*, *B*), KRS appears to bind preferentially to 67LR in the plasma membrane (Fig. 2*C*). It is not yet understood how KRS undergoes a conformational change to form a complex with 67LR in the membrane. Human KRS appears to exist as a homodimer that has a potential to form a homo- or heterotetramer (37). Because 67LR is formed by the dimerization of 37LRP (50), KRS and 67LR may form an $\alpha_2\beta_2$ or $\alpha_4\beta_2$ complex. The T52D mutation did not appear to change the homodimer formation of KRS (data not shown), implying that KRS may remain a dimer after being phosphorylated at T52. KRS binds only to the region containing both extracellular and transmembrane domains (Fig. 2*H*). Perhaps the binding of KRS to each separate domain is not strong enough or KRS binds specifically to the junction region between extracellular and transmembrane domains. Although it is not yet clear whether KRS can be located high enough to cover all 67LR, at least cells would have enough intracellular pool of KRS because it is a housekeeping enzyme for protein synthesis. All of these remaining questions call for further detailed investigation.

Post-translational modification was shown to be responsible for the control of association/dissociation of a few different components in MSC. For instance, phosphorylated EPRS is detached from MSC by IFN-γ treatment for translational silencing of the target transcripts (51). GCN2-dependent phosphorylation of MRS releases the bound tumor suppressor, AIMP3/p18, to repair DNA damage (52). Among the nonenzymatic components, phosphorylated AIMP2 is translocated into nucleus on DNA damage for the activation of p53 (53), and JNK-dependent phosphorylation of AIMP1 is involved in the control of its interaction with gp96 (54). These results indicate that MSC components, when dissociated from MSC, would respond specifically to different cellular stimuli through differential phosphorylation and execute their unique activities while they work together for protein synthesis when they are bound to MSC.

Although the biogenesis and physiological implication of 67LR are not yet completely understood, the increased level of 67LR has been acknowledged as a signature for metastatic cancer (19, 55–58). However, the regulator and molecular mechanism for the membrane stability of 67LR were not determined. Here we identified KRS as a positive regulator for 67LR and its effect on cell migration. It remains to be seen whether the effect of these two translational components on cell

migration is also recapitulated *in vivo* and applied to the metastatic behavior of cancer. FJ

This work was supported by Global Frontier (NRF-M1AXA002-2010-0029785), Acceleration Research (R17-2007-020-01000-0), and 21st Frontier Functional Proteomics Research (M108KM010027-08K1301-02710) grants from the National Research Foundation, funded by the Ministry of Education, Science, and Technology of Korea.

REFERENCES

1. Guo, M., Schimmel, P., and Yang, X. L. (2010) Functional expansion of human tRNA synthetases achieved by structural inventions. *FEBS Lett.* **584,** 434–442
2. Park, S. G., Ewalt, K. L., and Kim, S. (2005) Functional expansion of aminoacyl-tRNA synthetases and their interacting factors: new perspectives on housekeepers. *Trends Biochem. Sci.* **30,** 569–574
3. Park, S. G., Schimmel, P., and Kim, S. (2008) Aminoacyl tRNA synthetases and their connections to disease. *Proc. Natl. Acad. Sci. U. S. A.* **105,** 11043–11049
4. Kim, S., You, S., and Hwang, D. (2011) Aminoacyl-tRNA synthetases and tumorigenesis: more than housekeeping. *Nat. Rev. Cancer* **11,** 708–718
5. Lee, S. W., Kang, Y. S., and Kim, S. (2006) Multi-functional proteins in tumorigenesis: aminoacyl-tRNA synthetases and translational components. *Curr. Proteomics* **3,** 15
6. Park, S. G., Choi, E. C., and Kim, S. (2010) Aminoacyl-tRNA synthetase-interacting multifunctional proteins (AIMPs): a triad for cellular homeostasis. *IUBMB Life* **62,** 296–302
7. Lee, S. W., Cho, B. H., Park, S. G., and Kim, S. (2004) Aminoacyl-tRNA synthetase complexes: beyond translation. *J. Cell Sci.* **117,** 3725–3734
8. Han, J. M., Kim, J. Y., and Kim, S. (2003) Molecular network and functional implications of macromolecular tRNA synthetase complex. *Biochem. Biophys. Res. Commun.* **303,** 985–993
9. Han, J. M., Lee, M. J., Park, S. G., Lee, S. H., Razin, E., Choi, E. C., and Kim, S. (2006) Hierarchical network between the components of the multi-tRNA synthetase complex: implications for complex formation. *J. Biol. Chem.* **281,** 38663–38667
10. Ray, P. S., Arif, A., and Fox, P. L. (2007) Macromolecular complexes as depots for releasable regulatory proteins. *Trends Biochem. Sci.* **32,** 158–164
11. Halwani, R., Cen, S., Javanbakht, H., Saadatmand, J., Kim, S., Shiba, K., and Kleiman, L. (2004) Cellular distribution of lysyl-tRNA synthetase and its interaction with Gag during human immunodeficiency virus type 1 assembly. *J. Virol.* **78,** 7553–7564
12. Yannay-Cohen, N., Carmi-Levy, I., Kay, G., Yang, C. M., Han, J. M., Kemeny, D. M., Kim, S., Nechushtan, H., and Razin, E. (2009) LysRS serves as a key signaling molecule in the immune response by regulating gene expression. *Mol. Cell* **34,** 603–611
13. Park, S. G., Kim, H. J., Min, Y. H., Choi, E. C., Shin, Y. K., Park, B. J., Lee, S. W., and Kim, S. (2005) Human lysyl-tRNA synthetase is secreted to trigger proinflammatory response. *Proc. Natl. Acad. Sci. U. S. A.* **102,** 6356–6361
14. Roesli, C., Borgia, B., Schliemann, C., Gunthert, M., Wunderli-Allenspach, H., Giavazzi, R., and Neri, D. (2009) Comparative analysis of the membrane proteome of closely related metastatic and nonmetastatic tumor cells. *Cancer Res.* **69,** 5406–5414
15. Yan, W., Lee, H., Deutsch, E. W., Lazaro, C. A., Tang, W., Chen, E., Fausto, N., Katze, M. G., and Aebersold, R. (2004) A dataset of human liver proteins identified by protein profiling via isotope-coded affinity tag (ICAT) and tandem mass spectrometry. *Mol. Cell. Proteomics* **3,** 1039–1041
16. Yan, W., Lee, H., Yi, E. C., Reiss, D., Shannon, P., Kwieciszewski, B. K., Coito, C., Li, X. J., Keller, A., Eng, J., Galitski, T., Goodlett, D. R., Aebersold, R., and Katze, M. G. (2004) System-based proteomic analysis of the interferon response in human liver cells. *Genome Biol.* **5,** R54
17. Ardini, E., Pesole, G., Tagliabue, E., Magnifico, A., Castronovo, V., Sobel, M. E., Colnaghi, M. I., and Menard, S. (1998) The 67-kDa laminin receptor originated from a ribosomal protein that acquired a dual function during evolution. *Mol. Biol. Evol.* **15,** 1017–1025
18. Auth, D., and Brawerman, G. (1992) A 33-kDa polypeptide with homology to the laminin receptor: component of translation machinery. *Proc. Natl. Acad. Sci. U. S. A.* **89,** 4368–4372
19. Nelson, J., McFerran, N. V., Pivato, G., Chambers, E., Doherty, C., Steele, D., and Timson, D. J. (2008) The 67 kDa laminin receptor: structure, function and role in disease. *Biosci. Rep.* **28,** 33–48
20. Wewer, U. M., Taraboletti, G., Sobel, M. E., Albrechtsen, R., and Liotta, L. A. (1987) Role of laminin receptor in tumor cell migration. *Cancer Res.* **47,** 5691–5698
21. Donaldson, E. A., McKenna, D. J., McMullen, C. B., Scott, W. N., Stitt, A. W., and Nelson, J. (2000) The expression of membrane-associated 67-kDa laminin receptor (67LR) is modulated in vitro by cell-contact inhibition. *Mol. Cell. Biol. Res. Commun.* **3,** 53–59
22. Kim, W. H., Lee, B. L., Jun, S. H., Song, S. Y., and Kleinman, H. K. (1998) Expression of 32/67-kDa laminin receptor in laminin adhesion-selected human colon cancer cell lines. *Br. J. Cancer* **77,** 15–20
23. Nikles, D., Vana, K., Gauczynski, S., Knetsch, H., Ludewigs, H., and Weiss, S. (2008) Subcellular localization of prion proteins and the 37 kDa/67 kDa laminin receptor fused to fluorescent proteins. *Biochim. Biophys. Acta* **1782,** 335–340
24. Yung, Y., Yao, Z., Aebersold, D. M., Hanoch, T., and Seger, R. (2001) Altered regulation of ERK1b by MEK1 and PTP-SL and modified Elk1 phosphorylation by ERK1b are caused by abrogation of the regulatory C-terminal sequence of ERKs. *J. Biol. Chem.* **276,** 35280–35289
25. Naoghare, P. K., Ki, H. A., Paek, S. M., Tak, Y. K., Suh, Y. G., Kim, S. G., Lee, K. H., and Song, J. M. (2010) Simultaneous quantitative monitoring of drug-induced caspase cascade pathways in carcinoma cells. *Integr. Biol. (Camb.)* **2,** 46–57
26. Naoghare, P. K., Kim, M. J., and Song, J. M. (2008) Uniform threshold intensity distribution-based quantitative multivariate imaging cytometry. *Anal. Chem.* **80,** 5407–5417
27. Gagnoux-Palacios, L., Dans, M., van't Hof, W., Mariotti, A., Pepe, A., Meneguzzi, G., Resh, M. D., and Giancotti, F. G. (2003) Compartmentalization of integrin α6β4 signaling in lipid rafts. *J. Cell Biol.* **162,** 1189–1196
28. Yang, X. W. H., Flores, L. M., Li, Q. L., Zhou, P. C., Xu, F. H., Krop, I. E., and Hemler, M. E. (2010) Disruption of laminin-integrin-CD151-focal adhesion kinase axis sensitizes breast cancer cells to ErbB2 antagonists. *Cancer Res.* **70,** 2256–2263
29. Suh, H. N., and Han, H. J. (2010) Laminin regulates mouse embryonic stem cell migration: involvement of Epac1/Rap1 and Rac1/cdc42. *Am. J. Physiol. Cell Physiol.* **298,** C1159–C1169
30. Schlaepfer, D. D., and Mitra, S. K. (2004) Multiple connections link FAK to cell motility and invasion. *Curr. Opin. Genet. Dev.* **14,** 92–101
31. Grisaru-Granovsky, S., Salah, Z., Maoz, M., Pruss, D., Beller, U., and Bar-Shavit, R. (2005) Differential expression of protease activated receptor 1 (Par1) and pY397FAK in benign and malignant human ovarian tissue samples. *Int. J. Cancer* **113,** 372–378
32. Brunton, V. G., Avizienyte, E., Fincham, V. J., Serrels, B., Metcalf, C. A., 3rd, Sawyer, T. K., and Frame, M. C. (2005) Identification of Src-specific phosphorylation site on focal adhesion kinase: dissection of the role of Src SH2 and catalytic functions and their consequences for tumor cell behavior. *Cancer Res.* **65,** 1335–1342
33. Givant-Horwitz, V., Davidson, B., and Reich, R. (2005) Laminin-induced signaling in tumor cells. *Cancer Lett.* **223,** 1–10
34. Rho, S. B., Kim, M. J., Lee, J. S., Seol, W., Motegi, H., Kim, S., and Shiba, K. (1999) Genetic dissection of protein-protein interactions in multi-tRNA synthetase complex. *Proc. Natl. Acad. Sci. U. S. A.* **96,** 4488–4493
35. Kim, J. Y., Kang, Y. S., Lee, J. W., Kim, H. J., Ahn, Y. H., Park, H., Ko, Y. G., and Kim, S. (2002) p38 is essential for the assembly and stability of macromolecular tRNA synthetase complex: implications for its physiological significance. *Proc. Natl. Acad. Sci. U. S. A.* **99,** 7912–7916
36. Quevillon, S., Robinson, J. C., Berthonneau, E., Siatecka, M., and Mirande, M. (1999) Macromolecular assemblage of aminoacyl-tRNA synthetases: identification of protein-protein interactions and characterization of a core protein. *J. Mol. Biol.* **285,** 183–195

37. Guo, M., Ignatov, M., Musier-Forsyth, K., Schimmel, P., and Yang, X. L. (2008) Crystal structure of tetrameric form of human lysyl-tRNA synthetase: implications for multisynthetase complex formation. *Proc. Natl. Acad. Sci. U. S. A.* **105,** 2331–2336
38. Landowski, T. H., Dratz, E. A., and Starkey, J. R. (1995) Studies of the structure of the metastasis-associated 67 kDa laminin binding protein: fatty acid acylation and evidence supporting dimerization of the 32 kDa gene product to form the mature protein. *Biochemistry* **34,** 11276–11287
39. Buto, S., Tagliabue, E., Ardini, E., Magnifico, A., Ghirelli, C., van den Brule, F., Castronovo, V., Colnaghi, M. I., Sobel, M. E., and Menard, S. (1998) Formation of the 67-kDa laminin receptor by acylation of the precursor. *J. Cell. Biochem.* **69,** 244–251
40. Barczyk, M., Carracedo, S., and Gullberg, D. (2010) *Integrins Cell Tissue Res.* **339,** 269–280
41. Nguyen, B. P., Gil, S. G., and Carter, W. G. (2000) Deposition of laminin 5 by keratinocytes regulates integrin adhesion and signaling. *J. Biol. Chem.* **275,** 31896–31907
42. Xia, Y., and Karin, M. (2004) The control of cell motility and epithelial morphogenesis by Jun kinases. *Trends Cell Biol.* **14,** 94–101
43. Fujimura, Y., Yamada, K., and Tachibana, H. (2005) A lipid raft-associated 67 kDa laminin receptor mediates suppressive effect of epigallocatechin-3-O-gallate on Fc epsilon RI expression. *Biochem. Biophys. Res. Commun.* **336,** 674–681
44. Lafont, F., and Simons, K. (2001) Raft-partitioning of the ubiquitin ligases Cbl and Nedd4 upon IgE-triggered cell signaling. *Proc. Natl. Acad. Sci. U. S. A.* **98,** 3180–3184
45. Yasuda, J., Nakao, M., Kawaoka, Y., and Shida, H. (2003) Nedd4 regulates egress of Ebola virus-like particles from host cells. *J. Virol.* **77,** 9987–9992
46. Rotin, D., and Kumar, S. (2009) Physiological functions of the HECT family of ubiquitin ligases. *Nat. Rev. Mol. Cell Biol.* **10,** 398–409
47. Lukk, M., Kapushesky, M., Nikkila, J., Parkinson, H., Goncalves, A., Huber, W., Ukkonen, E., and Brazma, A. (2010) A global map of human gene expression. *Nat. Biotechnol.* **28,** 322–324
48. Hippo, Y., Taniguchi, H., Tsutsumi, S., Machida, N., Chong, J. M., Fukayama, M., Kodama, T., and Aburatani, H. (2002) Global gene expression analysis of gastric cancer by oligonucleotide microarrays. *Cancer Res.* **62,** 233–240
49. Sun, L., Hui, A. M., Su, Q., Vortmeyer, A., Kotliarov, Y., Pastorino, S., Passaniti, A., Menon, J., Walling, J., Bailey, R., Rosenblum, M., Mikkelsen, T., and Fine, H. A. (2006) Neuronal and glioma-derived stem cell factor induces angiogenesis within the brain. *Cancer Cell* **9,** 287–300
50. Jamieson, K. V., Wu, J., Hubbard, S. R., and Meruelo, D. (2008) Crystal structure of the human laminin receptor precursor. *J. Biol. Chem.* **283,** 3002–3005
51. Arif, A., Jia, J., Mukhopadhyay, R., Willard, B., Kinter, M., and Fox, P. L. (2009) Two-site phosphorylation of EPRS coordinates multimodal regulation of noncanonical translational control activity. *Mol. Cell* **35,** 164–180
52. Kwon, N. H., Kang, T., Lee, J. Y., Kim, H. H., Kim, H. R., Hong, J., Oh, Y. S., Han, J. M., Ku, M. J., Lee, S. Y., and Kim, S. (2011) Dual role of methionyl-tRNA synthetase in the regulation of translation and tumor suppressor activity of aminoacyl-tRNA synthetase-interacting multifunctional protein-3. *Proc. Natl. Acad. Sci. U. S. A.* **108,** 19635–19640
53. Han, J. M., Park, B. J., Park, S. G., Oh, Y. S., Choi, S. J., Lee, S. W., Hwang, S. K., Chang, S. H., Cho, M. H., and Kim, S. (2008) AIMP2/p38, the scaffold for the multi-tRNA synthetase complex, responds to genotoxic stresses via p53. *Proc. Natl. Acad. Sci. U. S. A.* **105,** 11206–11211
54. Kim, G., Han, J. M., and Kim, S. (2010) Toll-like receptor 4-mediated c-Jun N-terminal kinase activation induces gp96 cell surface expression via AIMP1 phosphorylation. *Biochem. Biophys. Res. Commun.* **397,** 100–105
55. Narumi, K., Inoue, A., Tanaka, M., Isemura, M., Shimo-Oka, T., Abe, T., Nukiwa, T., and Satoh, K. (1999) Inhibition of experimental metastasis of human fibrosarcoma cells by anti-recombinant 37-kDa laminin binding protein antibody. *Jpn. J. Cancer Res.* **90,** 425–431
56. Menard, S., Tagliabue, E., and Colnaghi, M. I. (1998) The 67 kDa laminin receptor as a prognostic factor in human cancer. *Breast Cancer Res. Treat.* **52,** 137–145
57. Castronovo, V. (1993) Laminin receptors and laminin-binding proteins during tumor invasion and metastasis. *Invasion Metastasis* **13,** 1–30
58. Liotta, L. A., Rao, N. C., Barsky, S. H., and Bryant, G. (1984) The laminin receptor and basement membrane dissolution: role in tumour metastasis. *Ciba Found. Symp.* **108,** 146–162

Received for publication March 22, 2012.
Accepted for publication June 11, 2012.